Seewald, Jeffrey S. ; Reeves, Eoghan P. ; Bach, Wolfgang ; Saccocia, Peter J. ; Craddock, Paul R. ; Shanks, Wayne C. ; Sylva, Sean P. ; Pichler, Thomas ; Rosner, Martin ; Walsh, Emily

Submarine venting of magmatic volatiles in the Eastern Manus Basin, Papua New Guinea

Submarine venting of magmatic volatiles in the Eastern Manus Basin, Papua New Guinea

Jeffrey S. Seewald [a,*], Eoghan P. Reeves [a,b], Wolfgang Bach [b], Peter J. Saccocia [c], Paul R. Craddock [a], Wayne C. Shanks III [d], Sean P. Sylva [a], Thomas Pichler [b], Martin Rosner [e], Emily Walsh [c]

[a] *Department of Marine Chemistry and Geochemistry, Woods Hole Oceanographic Institution, MS #4, Woods Hole, MA 02543, USA*
[b] *MARUM Center for Marine Environmental Sciences and Department of Geosciences, University of Bremen, Klagenfurter Str., 28359 Bremen, Germany*
[c] *Department of Geological Sciences, Bridgewater State University, Bridgewater, MA 02325, USA*
[d] *U.S. Geological Survey, 973 Denver Federal Center, Denver, CO 80225, USA*
[e] *Federal Institute of Materials Research and Testing, Unter den Eichen 87, 12205 Berlin, Germany*

1. INTRODUCTION

Submarine hot-spring fluids contain abundant magmatic volatiles that can fundamentally influence fluid–rock reactions and promote chemical exchange between the

* Corresponding author. Tel.: +1 (508) 289 2966.
E-mail address: jseewald@whoi.edu (J.S. Seewald).

lithosphere and overlying water column. In back-arc and submarine arc hydrothermal environments, spatial and temporal variability in crustal composition, abundance and composition of magmatic volatiles, subduction and mantle dynamics, magmatic activity, and seafloor morphology result in a broad range of hydrothermal fluid compositions. All of these factors are influenced by the subducting slab and vary systematically with increasing distance from the arc as the depth of subduction increases (Sinton et al., 2003; Pearce and Stern, 2006; Martinez et al., 2006; Bezos et al., 2009; Escrig et al., 2009; Mottl et al., 2011; Reeves et al., 2011). In the Manus back-arc basin, for example, the Vienna Woods hydrothermal system is hosted in basaltic crust where back-arc rifting and crustal generation is fully developed along the Manus spreading center located 250 km from the New Britain arc. At this location, magmatic volatiles in seawater-derived vent fluids are dominated by CO_2 with no evidence for significant H_2O or SO_2 contributions (Reeves et al., 2011), similar to mid-ocean ridge settings characterized by basaltic magmatism (Lilley et al., 2003; Shanks et al., 1995). Further to the east at the PACMANUS, DESMOS, and SuSu Knolls hydrothermal areas, hot-springs are hosted in more felsic crust within an extensional transform zone that lacks a clearly-defined spreading center. Located $\leqslant$100 km from the active New Britain arc, the influence of the subducting slab on hydrothermal fluid chemistry is readily apparent in the composition of dissolved volatiles. In addition to CO_2, magmatic degassing is thought to contribute significant quantities of H_2O, SO_2, and HF to PACMANUS and DESMOS vent fluids (Gamo et al., 1997; Gena et al., 2006; Reeves et al., 2011). Because SO_2 disproportionation to sulfuric acid (Iwasaki and Ozawa, 1960; Holland, 1965; Kusakabe et al., 2000) and direct addition of other acidic magmatic volatiles such as HCl represent abundant sources of strong acids, magmatic degassing in these environments significantly influences the mineralogy and composition of crustal alteration assemblages and the transport of metals in solution.

The contribution of magmatic fluids to hydrothermal fluid chemistry has received much attention in the context of ore-deposit formation (e.g., Hedenquist and Lowenstern, 1994; de Ronde, 1995; Heinrich, 2005; Yang and Scott, 2006). It has been suggested that magmatic fluids may contain levels of magma-derived ore-forming metals that are sufficient to account for the quantities of metals observed in seafloor mineral deposits and may represent the source of metals in hydrothermal fluids responsible for ore formation (Yang and Scott, 1996, 2002). Magmatic fluids have also been invoked as a source of acidity and complexing ligands to hydrothermal fluids that may efficiently leach ore-forming metals from surrounding crustal rocks prior to concentration at the site of deposition (Hedenquist and Lowenstern, 1994). Recent studies have suggested that acidic magmatic volatiles may contribute to metal mobilization in seawater-derived metal-rich black-smoker fluids venting in arc and back-arc environments (de Ronde et al., 2005; Embley et al., 2006; Resing et al., 2007; Takai et al., 2008; de Ronde et al., 2011; Mottl et al., 2011; Reeves et al., 2011). Although these fluids show a clear magmatic contribution, the composition of the magmatic fluid prior to mixing with the convectively circulating seawater-derived component and its role during metal mobilization is obscured by subsequent fluid–rock interaction and phase separation processes.

Magmatic volatiles have been identified in highly acidic SO_4-rich low temperature white smoker fluids venting from the back-arc DESMOS vent field and the NW Rota-1 and Brothers intraoceanic arc volcanos (Gamo et al., 1997; Gena et al., 2006; Resing et al., 2007; Butterfield et al., 2011; de Ronde et al., 2011). These acid-sulfate fluids represent a very different style of hydrothermal activity compared to high temperature black-smoker fluids that have been studied extensively at oceanic-spreading centers. In particular, they are more acidic and contain substantially higher aqueous SO_4 and Mg concentrations relative to black-smoker fluids, sharing similarities with the fluids responsible for high sulfidation deposits in subaerial settings (Hedenquist and Lowenstern, 1994). While numerous hydrothermal systems with this type of venting are now known to exist in back-arc and intraoceanic arc environments (Gamo et al., 1997; Butterfield et al., 2011; de Ronde et al., 2011; Leybourne et al., 2012), compositional information is limited and their temporal variability has only been observed indirectly through changes in water column plume chemistry (de Ronde et al., 2003, 2005). Because their chemistry appears to be highly influenced by the abundant presence of magmatic volatiles, they can provide new insight into the composition of magmatic fluids involved in hydrothermal activity in submarine back-arc and arc settings, and their role in hydrothermal alteration and magma dynamics.

Here we report data for the composition of acid-sulfate fluids collected in 2006 from the SuSu Knolls and DESMOS vent fields located in the back-arc environment of the Eastern Manus Basin. The compositions of fluids from the SuSu Knolls vent area have not been reported previously and greatly expand the range of observations that can be used to constrain physical and chemical processes associated with submarine acid-sulfate venting. The DESMOS area was previously sampled on several occasions between 1995 and 2000 (Gamo et al., 2006 and references therein). The data presented here augment these earlier studies by providing additional information regarding the temporal evolution of acid-sulfate venting. Information regarding the abundance of dissolved gases along with non-volatile aqueous species are used to assess the composition of magmatic fluids released from subseafloor magmatic bodies, processes controlling the formation and composition of acid-sulfate fluids in back-arc environments, and resulting chemical exchange between the lithosphere and water column.

2. GEOLOGIC SETTING

The Manus Basin (Fig. 1), located in the northeastern Bismarck Sea, is a young (ca. 3.5 Ma) back-arc basin that is rapidly opening at full rates up to 137 mm/y (Tregoning, 2002). It is bordered to the north by the presently inactive Manus Trench and to the south by the active

New Britain Trench (Taylor, 1979a; Taylor et al., 1994; Lee and Ruellan, 2006). Volcanism associated with basin extension occurs along a series of spreading centers and rifts between three major transform faults (Taylor, 1979a; Taylor et al., 1994; Martinez and Taylor, 1996). Fully-developed spreading in the center of the basin occurs along the 120 km-long Manus Spreading Center, which hosts the unsedimented Vienna Woods hydrothermal field (Both et al., 1986; Tufar, 1990; Lisitsyn et al., 1993; Reeves et al., 2011) in predominantly MORB-like basalt. In contrast, the Eastern Manus Basin between the Djaul and Weitin transform faults is an extensional transform zone within remnant Eocene–Oligocene island-arc crust that is thought to have formed during previous southwestward subduction along the Manus Trench (Binns and Scott, 1993; Binns et al., 2007). Volcanism associated with the incipient rifting of pre-existing intermediate/felsic crust has produced a complex series of *en echelon* neovolcanic seafloor ridges and domes collectively known as the Eastern Manus Volcanic Zone (Fig. 1). The composition of these edifices varies from basaltic to rhyodacitic compositions (Binns and Scott, 1993; Kamenetsky et al., 2001; Sinton et al., 2003) and they possess isotopic, major, and trace element characteristics similar to subaerial volcanoes of the New Britain Arc, indicating strong arc affinities (Sinton et al., 2003; Pearce and Stern, 2006). Due to its proximity to the New Britain Arc (<100 km), the relative influences of the mantle wedge, subducting slab and remnant arc crust on melt production, and volcanism in the Eastern Manus volcanic zone are complex (Sinton et al., 2003; Pearce and Stern, 2006). During the last two decades, areas of hydrothermal activity have been discovered in the Eastern Manus volcanic zone (Fig. 1), including the DESMOS caldera, the SuSu Knolls area, and the PACMANUS and Northeast Pual sites located on Pual Ridge (Binns and Scott, 1993; Gamo et al., 1993, 1997, 2006; Auzende et al., 1997, 2000; Binns et al., 1997; Gena et al., 2001, 2006; Moss and Scott, 2001; Tivey et al., 2006; Hrischeva et al., 2007; Craddock et al., 2010; Reeves et al., 2011).

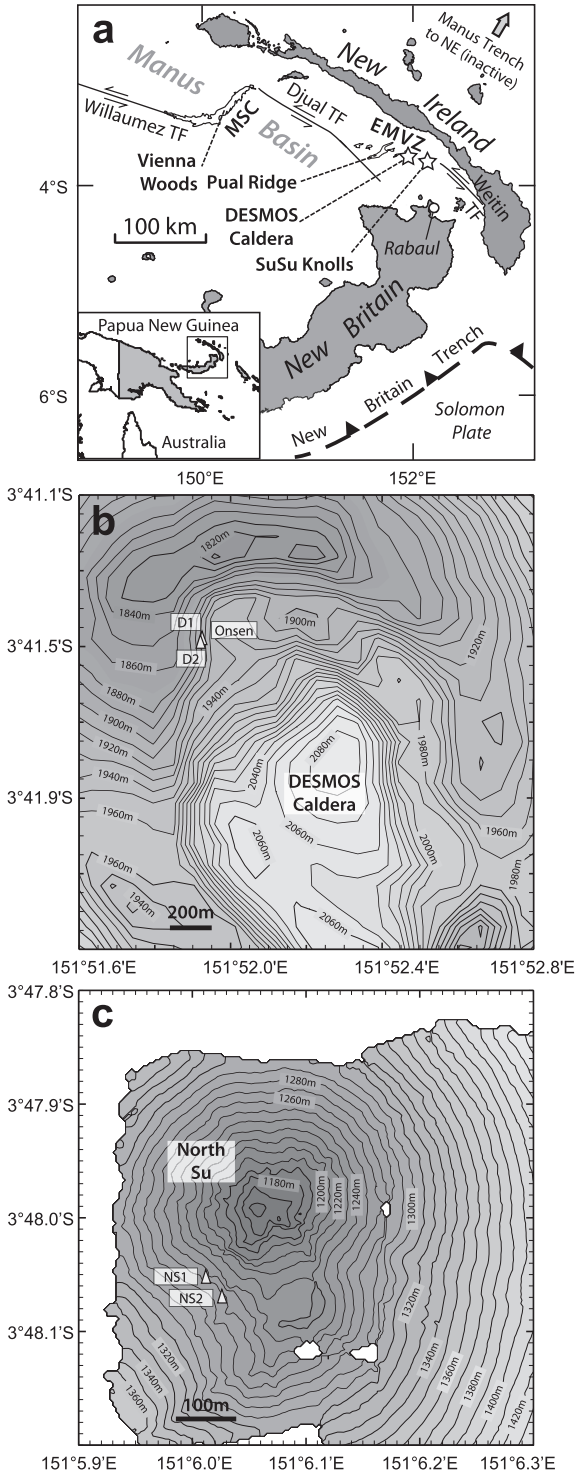

Fig. 1. Maps showing the location of (a) the Manus Basin relative to the New Britain and New Ireland arcs, (b) fluids sampled from the DESMOS caldera, and (c) fluids sampled from North Su volcano (adapted from Tivey et al., 2006). EMZV in (a) indicates the location of the Eastern Manus Volcanic Zone.

2.1. Hydrothermal vent fields

2.1.1. DESMOS caldera

The DESMOS neovolcanic edifice is an elongated NNW-trending caldera rising to ~1810 m depth with a width of 1.5–2 km and a caldera depression of 150–250 m (Fig. 1b). The seafloor within the caldera consists of fresh basaltic andesite pillow lavas, changing to hyaloclastite deposits of both altered and unaltered basaltic andesite clasts on the northern caldera wall (Gena et al., 2001, 2006; Tivey et al., 2006). In some cases, recent pillow flows cover hyaloclastite talus and, in general, sediment cover is minor to negligible (Tivey et al., 2006). Buoyant hydrothermal plumes discovered in 1990 provided the first evidence for hot-spring activity at this site (Gamo et al., 1993). In 1995, venting of milky white smoker fluids (88–120 °C) at the Onsen site was documented on a ledge of the northern wall (Gamo et al., 1997, 2006). The milky white precipitate characteristic of this venting was shown to be elemental sulfur (Gena et al., 2006). Previous studies have collected fluid samples in 1995, 1996, 1998, 1999, and 2000 (Auzende et al., 1996, 1997; Gamo et al., 1996b, 1997, 2006;

Douville et al., 1999a,b; Gena et al., 2001, 2006; Fourre et al., 2006). Fluids samples were collected during this study at two sites (D1 and D2; Fig. 1b) at a depth of 1910 m from the area of venting that was approximately 30 m in diameter in 2006. The seafloor expression of hydrothermal activity is manifest as poorly focused venting of white smoker fluids with measured exit temperatures of 70–117 °C from small flange-like deposits composed of native sulfur and from sulfur-cemented, highly bleached hyaloclastite talus with a notable absence of sulfide structures or deposits.

2.1.2. North Su

The North Su site (Fig. 1c) is located on a dacitic, neovolcanic dome that rises to a water depth of 1160 m within the SuSu Knolls series of hydrothermally-active neovolcanic edifices that overlie the older andesitic Tumai Ridge (Binns et al., 1997; Auzende et al., 2000; Moss and Scott, 2001; Tivey et al., 2006; Hrischeva et al., 2007). Unlike DESMOS, no caldera is present on the North Su dome. The entire series of SuSu Knolls edifices is covered with a sediment apron of variable thickness (up to several meters) consisting of layered, dark and locally sulfidic sandy sediment that is most likely a mixture of volcanoclastic and pelagic/hemipelagic material, based on the compositions of adjacent Suzette area sediments investigated by Hrischeva et al. (2007). A large complex of black smokers up to 11 m high venting fluids with variable temperatures $\leqslant$325 °C is present on the summit of the North Su dome (these fluids are not discussed here). The flanks of the dome host numerous white smoker vents that are very similar in nature to DESMOS, but substantially more abundant and vigorous with measured exit temperatures of 48–215 °C. The white smoker fluids typically vent from talus piles consisting of extensively altered volcanic clasts, but in some cases from areas with minor hydrothermal sediment cover, and flows and flanges of native sulfur are common nearby. In areas of more substantial hydrothermal sediment cover on the dome flanks, molten sulfur at temperatures of 272–284 °C was recovered less than 0.5 m beneath the sediment–water interface. Several large lava spines protrude up to 15 m from the hydrothermal detritus and diffuse venting was observed around the base of these structures. Fluids samples were collected from two locations (NS1 and NS2; Fig. 1c) at 1160 m water depth.

3. METHODS

White smoker vent fluids were collected using isobaric gas-tight fluid samplers (Seewald et al., 2002) and syringe style 'major' samplers (Von Damm et al., 1985) deployed from the ROV *Jason* II. At each vent, two separate samples were collected using the gas-tight samplers (IGT-prefix, Table 1) and a third sample was collected using the 'major' sampler (M-prefix, Table 1). Vent fluid temperature was monitored continuously during fluid sampling using a thermocouple attached to the end of the sampler inlet snorkel. The reported temperatures (Table 1) represent maximum values recorded during collection of each sample with an estimated uncertainty of ±2 °C.

Fluid samples were processed on the ship within 24 h of recovery. Shipboard measurements of pH (25 °C) were made using a Ag/AgCl combination reference electrode that was calibrated daily. Dissolved H_2 and CH_4 abundances were determined shipboard following a headspace extraction using a gas chromatograph equipped with a 5 Å molecular sieve packed column and a thermal conductivity detector. Total aqueous sulfide ($\Sigma H_2S = H_2S + HS^- + S^{2-}$) was sparged from a sample aliquot acidified with 25 wt.% phosphoric acid and precipitated shipboard as Ag_2S in a 5 wt.% solution of $AgNO_3$ for subsequent gravimetric measurement in a shore-based laboratory.

For each sample, several aliquots were stored in acid cleaned high density polyethylene bottles for shore-based analysis. One aliquot was sparged at sea for approximately 30 min with ultra-high purity N_2 gas prior to storage to remove volatile sulfur species such as H_2S and SO_2 that may oxidize during storage and contribute to the measured total dissolved sulfate concentration ($\Sigma SO_4 = SO_4^{2-} + HSO_4^- + H_2SO_4$). Major anions (Cl, ΣSO_4, Br, F) and cations (Na, K, Ca, Mg) were analyzed by ion chromatography with suppressed conductivity detection. Another aliquot was acidified with analytical-grade Optima® HCl prior to storage for trace metal analysis by inductively-coupled plasma mass spectrometry (ICP-MS) and inductively-coupled plasma atomic emission spectroscopy (ICP-AES). A sub-sample of the acidified aliquot was diluted 100-fold (v/v) at sea for measurement of aqueous SiO_2 by ICP-AES. Samples of high temperature vent fluids typically contain transition metal-rich precipitates due to cooling and mixing with alkaline seawater during sampling (e.g., Trefry et al., 1994). These precipitates were collected on 0.45 μm nylon filters then dissolved and analyzed by ICP-MS, allowing reconstruction of fluid composition prior to precipitation. Several aliquots of fluid were stored in 30 mL serum vials with butyl-rubber stoppers for shore-based chemical and isotopic analysis of total dissolved carbonate ($\Sigma CO_2 = CO_3^{2-} + HCO_3^- + H_2CO_3$). Concentrations of dissolved ΣCO_2 were determined after acidification of fluids with 25 wt.% phosphoric acid by injecting aliquots of headspace gas directly into a gas chromatograph equipped with a Porapak-Q packed column and a thermal conductivity detector. These data were corrected to account for CO_2 partitioning between the headspace and fluid phase within the culture tube. Fluid aliquots were also flame-sealed in glass ampoules for stable hydrogen and oxygen isotope analysis. Estimates of overall maximum analytical uncertainties (2σ) are ±10% for H_2, CH_4, CO, ΣH_2S, Sr, Li, Rb, Cs, Fe, and Al concentrations, ±5% for ΣCO_2, Mn, Br, and F concentrations, ±3% for Na, Cl, Ca, K, and SO_4 concentrations, ±2% for SiO_2 concentrations, and ±0.02 units for pH (25 °C).

The stable carbon isotope composition of ΣCO_2 was determined by isotope ratio monitoring-gas chromatography mass spectrometry (irm-GCMS) using a Finnigan Delta^{Plus} XL mass spectrometer coupled to an Agilent 6890 gas chromatograph via a GCCIII combustion interface held at 950 °C with a constant oxygen trickle. The pooled standard deviation (1σ) for $\delta^{13}C_{CO_2}$ measurements is 0.3‰. The ^{34}S content of SO_4 in selected sparged fluid

Table 1
Measured concentrations[*] and isotopic composition of aqueous species and sulfur particles in vent fluids from the DESMOS and SuSu Knolls Vent Fields.

Sample	Vent	T_{max} °C	pH 25 °C	Mg mm	Na mm	K mm	Na/K molal	K/Mg molal	Na/Mg molal	Li μm	Rb μm	Cs nm	Ca mm	Ba μm	Sr μm	$^{87}Sr/^{86}Sr$ molal	Fe mm	Mn μm
DESMOS																		
J2-220-IGT1	D1	113	0.95	44.9	391	8.3	47	0.18	8.7	24	2.8	11	9.4	nd	71	0.70880	12.4	40
J2-220-IGT2	D1	117	0.95	45.1	392	8.4	47	0.19	8.7	25	3.3	9	9.4	nd	72	nd	11.9	37
J2-220-M4	D1	nd	1.27	50.0	438	9.2	48	0.18	8.8	29	0.8	8	9.8	nd	86	nd	5.62	28
J2-220-IGT4	D2	70	1.41	49.3	422	8.7	48	0.18	8.6	31	3.1	8	11.9	4	78	0.70886	5.56	46
J2-220-IGT3	D2	69	1.40	49.2	421	8.8	48	0.18	8.6	21	0.3	8	11.7	4	79	nd	5.46	46
J2-220-M2	D2	nd	1.41	49.4	419	8.8	48	0.18	8.5	25	1.0	11	11.9	nd	80	nd	5.53	43
North Su																		
J2-221-IGT8	NS1	47	1.87	50.4	453	10.0	45	0.20	9.0	30	0.7	33	9.7	11	85	0.70895	1.32	21
J2-221-IGT7	NS1	48	1.79	49.6	447	9.8	46	0.20	9.0	35	1.9	40	9.6	12	86	nd	1.63	26
J2-221-M4	NS1	nd	1.85	49.8	450	9.8	46	0.20	9.0	34	1.2	38	9.6	nd	87	nd	1.42	22
J2-221-IGT6	NS2	206	0.87	39.2	340	7.8	44	0.20	8.7	27	1.0	64	8.9	nd	58	0.70870	3.10	81
J2-221-IGT5	NS2	215	0.87	41.1	359	8.0	45	0.20	8.7	34	2.7	56	9.1	nd	64	nd	2.57	67
J2-221-M2	NS2	nd	0.91	41.1	359	8.0	45	0.19	8.7	34	1.5	56	9.0	nd	63	nd	2.47	68
Bottom Seawater		3	7.9	52.4	471	9.9	48	0.19	9.0	28	1.3[a]	2.3[a]	10.5	0.14	91	0.70916	0.0	0.0

Sample	Vent	Al mm	Cl mm	Br μm	F μm	ΣSO_4 mm	$\delta^{34}S_{SO_4}$ ‰	ΣSO_{4ns}[†] mm	SO_2[‡] mm	$\delta^{34}S_{part}$[♯] ‰	SiO_2 mM	H_2 μM	ΣH_2S mM	CH_4 μM	ΣCO_2 mm	$\delta^{13}C_{CO_2}$ ‰	$\delta^{18}O_{H_2O}$ ‰	δD_{H_2O} ‰
DESMOS																		
J2-220-IGT1	D1	0.48	492	610	137	125	nd	147	22	nd	8.32	3.3	0.005	0.13	23	nd	0.7	−4
J2-220-IGT2	D1	0.47	495	620	128	123	9.8	139	16	−5.2	7.90	4.8	0.004	0.09	21	−3.0	0.9	−5
J2-220-M4	D1	0.21	523	713	85		nd	80.0		−6.2	3.46	nd	nd	nd	nd	nd	nd	nd
J2-220-IGT4	D2	1.6	503	706	8	55.3	17.2	62.6	7	nd	5.66	2.6	0.35	0.02	11	−3.6	0.6	−3
J2-220-IGT3	D2	1.6	502	721	5	54.4	17.4	59.5	5	nd	5.65	1.7	0.41	0.02	11	nd	0.8	−3
J2-220-M2	D2	1.6	501	719	4		nd	61.7		nd	5.66	nd	nd	nd	nd	nd	nd	nd
North Su																		
J2-221-IGT8	NS1	0.18	527	787	46	35.3	nd	41.0	6	nd	3.04	11	0.50	0.39	16	nd	0.2	−4
J2-221-IGT7	NS1	0.21	520	774	55	37.4	nd	39.9	3	nd	3.66	12	0.63	0.40	20	−2.4	0.7	−1
J2-221-M4	NS1	0.21	524	781	47	nd	nd	40.2		nd	3.30	nd	nd	nd	nd	nd	nd	nd
J2-221-IGT6	NS2	1.1	443	510	128	132	15.2	149	17	−3.6	9.94	18	<0.002	0.64	82	nd	1.5	−5
J2-221-IGT5	NS2	0.93	456	559	103	120	15.3	130	10	−1.5	8.56	22	<0.002	0.54	74	−2.8	2.2	−8
J2-221-M2	NS2	0.94	457	550	90	nd	nd	132		−1.4	8.90	nd	nd	nd	nd	nd	nd	nd
Bottom Seawater		0.0	540	808	64	28.2	20.99[b]	–	–		0.13[c]	0.0	0.0	0.0	2.3	0.3[d]	−0.17[e]	−0.14[f]

[*] mM = mmol/L fluid, mm = mmol/kg fluid, μm = μmol/kg fluid, μM = μmol/L fluid, nm = nmol/kg fluid, nd = not determined.
[†] measured ΣSO_4 concentration in fluid aliquot that was not sparged with N_2 prior to storage (see text).
[‡] calculated as the difference between measured ΣSO_4 concentrations in sparged and unsparged fluid samples (see text).
[♯] sulfur isotopic composition of elemental sulfur particles filtered from fluid. Data from McDermott et al. (2015).
[a] Spencer et al. (1970).
[b] Rees et al. (1978).
[c] Sarmiento and Gruber (2006).
[d] Craig (1970).
[e] Craig and Gordon (1965).
[f] Redfield and Friedman (1965).

samples was determined using an automated elemental analyzer interfaced to an isotope ratio mass spectrometer following precipitation as $BaSO_4$. Analytical uncertainty for $\delta^{34}S$ values was $\pm 0.3‰$ (2σ). Oxygen isotope compositions of vent fluid H_2O were analyzed using an automated CO_2 equilibration device on a VG Optima mass spectrometer. Hydrogen isotope compositions of vent fluid H_2O were analyzed as H_2 on a Finnigan MAT 252 mass spectrometer. The Zn reduction technique (Kendall and Coplen, 1985) was used to prepare H_2 following salt removal by vacuum distillation. Analytical uncertainty (2σ) for δD_{H_2O} and $\delta^{18}O_{H_2O}$ values were estimated to be 3‰ and 0.2‰, respectively. $^{87}Sr/^{86}Sr$ ratios were determined on a subset of samples on a Finnigan MAT 261 thermal ionization mass spectrometer using static multi-collection (Eickmann et al., 2009). Analytical uncertainty for $^{87}Sr/^{86}Sr$ values is estimated at 0.00007 (2σ) based on three individually processed aliquots of IAPSO reference seawater. With the exception of $^{87}Sr/^{86}Sr$, all stable isotope data are reported using standard delta notation. For the isotope A of interest, δA is defined by the expression:

$$\delta A\,(‰) = \left[\frac{R_S - R_{STD}}{R_{STD}}\right] \times 1000$$

where R_S and R_{STD} are the isotope ratios of the sample and standard, respectively. $\delta^{13}C_{CO_2}$ and $\delta^{34}S_{SO_4}$ are expressed relative to the V-PDB and V-CDT scales, respectively, whereas $\delta^{18}O_{H_2O}$ and δD_{H_2O} values are expressed relative to the V-SMOW scale.

4. RESULTS

4.1. Major species and pH

In general, acid-sulfate fluids at DESMOS and North Su contain high levels of Mg that range from just below seawater concentrations to a minimum value of 39.2 mmol/kg in the NS2 vent fluid. Replicate samples from each vent yielded similar concentrations and temperatures indicating that the elevated Mg abundances reflect the composition of fluids exiting the seafloor rather than inadvertent entrainment of ambient seawater during sampling.

A striking feature of these fluids that is reflected in the term "acid-sulfate" is the extraordinarily low measured pH (25 °C) and elevated ΣSO_4 concentrations (Table 1). Measured pH (25 °C) values vary from 0.95 to 1.41 at DESMOS and 0.87 to 1.85 at North Su. These are among the lowest values of pH measured to date in seafloor hydrothermal systems. The low pH values are accompanied by measured ΣSO_4 abundances far in excess of seawater concentrations, varying from 54.4 to 125 mmol/kg at DESMOS and 35.3 to 132 mmol/kg at North Su. Measurement of aqueous ΣSO_4 in fluid aliquots that were not N_2-sparged at sea reveals concentrations that are higher by as much as 22 mmol/kg (Table 1). These higher concentrations cannot reflect H_2S oxidation during storage due to the very low ΣH_2S contents of these fluids (Table 1). It is likely that the excess ΣSO_4 concentrations measured in the non-sparged aliquots reflect oxidation of residual SO_2 and other associated intermediate oxidation state sulfur species (e.g., thiosulfate, Kusakabe et al., 2000) during the storage period of several months and the rapid kinetics of $SO_{2(aq)}$ oxidation at low pH in Fe- and Mn-bearing solutions (Huss et al., 1982). Assuming this to be the case, the abundance of SO_2 and associated species can be calculated from the difference in measured ΣSO_4 concentrations between the sparged and non-sparged samples. SO_2 concentrations estimated in this way vary from 3 to 22 mmol/kg (Table 1). These represent minimum values since no measures were taken to minimize degassing of volatile species during handling of the unsparged fluid aliquots.

Measured Cl concentrations in DESMOS and North Su acid-sulfate fluids are consistently depleted relative to seawater, varying from 492 to 523 mmol/kg at DESMOS and 443 to 527 mmol/kg at North Su. Similar depletions are observed in the measured Na concentrations that vary from 391 to 419 mmol/kg at DESMOS and 340 to 453 mmol/kg at North Su. Unlike the majority of ridge-crest hydrothermal fluids that are enriched in K relative to seawater (Von Damm, 1995; German and Von Damm, 2003), the DESMOS and North Su K concentrations show depletions at levels similar to that observed for Na and Cl, with concentrations ranging from 7.8 to 10 mmol/kg. Measured Ca concentrations, however, are characterized by both minor depletions and enrichments, varying from 8.9 to 12 mmol/kg. Aqueous SiO_2 concentrations are highly enriched in the acid-sulfate fluids relative to seawater varying from 3.0 to 9.9 mmol/L.

4.2. Trace elements

Measured concentrations of the alkali trace elements Li, Rb, and Cs in acid-sulfate fluids at DESMOS and SuSu Knolls are enriched relative to seawater (Table 1). Aqueous Cs concentrations show the greatest enrichment, varying from 8 to 64 nmol/kg relative to 2.3 nmol/kg in seawater, while Li and Rb show concentrations that are only slightly enriched or depleted relative to the seawater values of 28 and 1.3 μmol/kg, respectively.

Measured concentrations of Br are below seawater values (Table 1). Although the measured concentrations of aqueous Br correlate with aqueous Cl, Br/Cl ratios are at or below seawater values. Measured aqueous F concentrations show highly variable behavior, being depleted relative to seawater (64 μmol/kg) in the D2 and NS1 fluids with concentrations of 4 to 8 μmol/kg and 46 to 55 μmol/kg, respectively, while the D1 and NS2 fluids show enriched F concentrations of 85 to 137 μmol/kg and 90 to 128 μmol/kg, respectively.

Dissolved Fe concentrations in the acid-sulfate fluids vary from 5.46 to 12.4 mmol/kg at DESMOS and 1.32 to 3.10 mmol/kg at North Su. The high Fe concentrations are accompanied by high aqueous Al concentrations that vary from 0.21 to 1.6 mmol/kg at DESMOS and 0.18 to 1.1 mmol/kg at North Su. The high aqueous Fe and Al concentrations, notwithstanding, Mn concentrations are substantially lower, ranging from 28 to 46 μmol/kg at DESMOS and 21 to 81 μmol/kg at North Su.

4.3. Dissolved gases

DESMOS and North Su acid-sulfate fluids are characterized by measured H_2 concentrations that vary from 1.7 to 22 μmol/L (Table 1). The elevated H_2 concentrations are accompanied by dissolved ΣH_2S concentrations that vary from below detection (<0.002 mmol/L) to 0.63 mmol/L. Measured dissolved ΣCO_2 concentrations vary from 11 to 82 mmol/kg in the acid-sulfate fluids, while concentrations of dissolved CH_4 vary from 0.02 to 0.64 μmol/L.

4.4. H_2O, CO_2 and SO_4 isotopic composition

The isotopic composition of hydrogen and oxygen in H_2O, carbon in ΣCO_2, and sulfur in ΣSO_4 from the DESMOS and North Su fluids show substantial deviations from seawater values (Table 1). For H_2O, measured values of $\delta^{18}O$ vary from 0.2‰ to 2.2‰ while values of δD vary from −1‰ to −8‰. The measured carbon isotopic composition of ΣCO_2 ranges from −2.4‰ to −3.6‰. Measured $\delta^{34}S$ values for dissolved SO_4 are much lower than seawater (+20.99‰, Rees et al., 1978), ranging from +9.8‰ to +17.4‰.

5. DISCUSSION

Many aspects of the acid-sulfate fluid compositions in the Eastern Manus Basin show a resemblance to the composition of seawater, while other aspects are dramatically different. For example, abundances of Na, K, Mg, Cl and some trace alkalis show consistent small depletions relative to seawater concentrations, while acidity, ΣSO_4, ΣCO_2, H_2, Fe, Mn, and Al abundances are substantially enriched. Models for the formation and chemical evolution of black-smoker vent fluids observed at oceanic-spreading centers involve the convective circulation of seawater in the oceanic lithosphere. Conductive heating of seawater as it percolates downwards through permeable crustal pathways induces extensive chemical interaction with fresh rock at low water/rock ratios and, in many cases, phase separation that extensively modify the original seawater composition (Seyfried, 1987; Von Damm, 1995; Butterfield et al., 2003; German and Von Damm, 2003). The integrated effects of these processes produce fluids that are depleted in Mg and SO_4, moderately acidic (pH ≈ 3–4), and enriched in Ca, K, SiO_2, mobile trace elements, H_2, ΣH_2S, ΣCO_2, and sulfide-forming metals that ultimately vent at the seafloor at temperatures approaching 400 °C (Seyfried, 1987; Von Damm, 1995; German and Von Damm, 2003). The low temperatures and compositionally distinct nature of acid-sulfate fluids at DESMOS and SuSu Knolls strongly suggest that a fundamentally different model is necessary to explain their genesis. Here we present evidence that formation of these fluids does not involve thermal convection of seawater-derived hydrothermal fluids, but instead occurs via direct injection of aqueous and sulfurous magmatic fluids directly into seawater, and thus represents a submarine analog of subaerial fumaroles.

5.1. Origin of acid sulfate fluids

Considering the high porosity and permeability of shallow oceanic crust and the ubiquitous occurrence of seawater in submarine environments, the involvement of chemically unmodified seawater in the formation of acid-sulfate fluids at DESMOS and North Su is not surprising. In addition to concentrations of Na, K, and Mg that are at, or slightly below, seawater values, relative abundances of these species are similar to seawater, regardless of their absolute concentration. For example, molal Na/K, K/Mg, and Na/Mg ratios in the DESMOS and North Su fluids vary from 45 to 48, 0.18 to 0.20, and 8.5 to 9.0 and, within analytical error, are nearly identical to seawater values of 48, 0.19, and 9.0, respectively. This relationship is apparent in Fig. 2 where Na and K concentrations reveal linear trends that are consistent with a line drawn between seawater composition and the origin when plotted against Mg. These trends indicate that the extent of depletion for each species in a given fluid is the same relative to seawater and is consistent with their conservative behavior during seawater dilution by an aqueous fluid containing near zero concentrations of Na, K, and Mg. Although the possibility exists that mixing could involve a

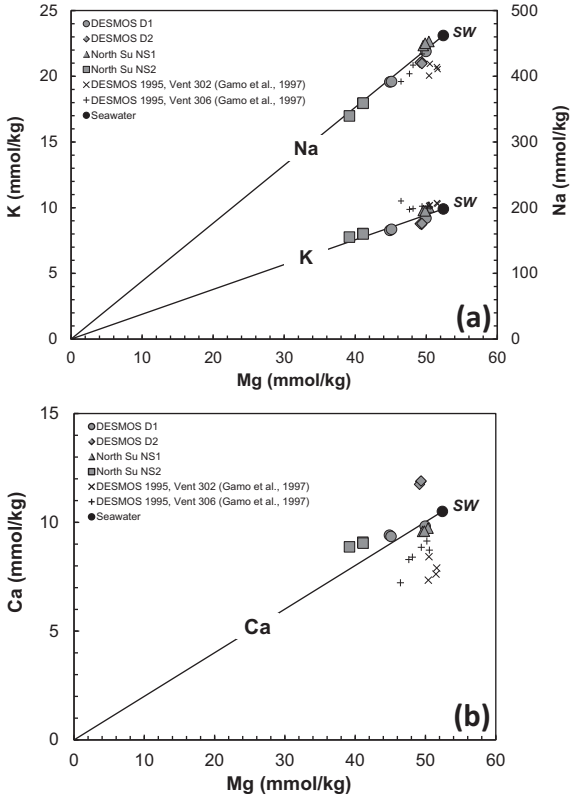

Fig. 2. Concentrations of selected aqueous species versus aqueous Mg in acid-sulfate vent fluids collected from the DESMOS and North Su vent areas in 2006. Concentrations measured at DESMOS in 1995 by Gamo et al. (1997) are shown for comparison. Lines drawn from seawater to the origin show the effect of dilution by pure water.

non-seawater fluid containing significant, but lower than seawater, concentrations of Na, K, and Mg, this scenario is unlikely since it would require that the relative abundances of all three species in the more dilute fluid were identical to seawater.

The most likely candidate for a fluid containing near-zero concentrations of Na, K, and Mg is a water-rich volatile phase degassing from an underlying magma chamber. Volumetrically significant, low salinity, volatile-rich magmatic fluids are predicted to form along with lesser volumes of high salinity brines during supercritical phase separation of NaCl-rich magmatic fluids released at magmatic temperatures and ambient pressures in the vicinity of shallow magma chambers (Gruen et al., 2014). Due to the lower density of the low salinity fluids relative to the higher density brines and seawater, they preferentially vent at the seafloor (Gruen et al., 2014). Thus, in contrast to processes responsible for the formation of black-smoker fluids, the model proposed here involves a high temperature endmember fluid that is entirely magmatic in origin and not the result of extensive chemical interaction between seawater and fresh rock during thermally driven convective circulation through oceanic crust. The formation of such fluids has been predicted by hydrodynamic models for hydrothermal activity in the vicinity of volatile-rich silicic magmas associated with arc-volcanism (Gruen et al., 2014). Reaction of magmatic fluids with crustal rocks during ascent before and after mixing with cold seawater may affect the abundance of some chemical species while leaving others unchanged. Based on the minimum measured Mg concentrations at each vent and the assumption of conservative mixing of a zero-Mg magmatic fluid and seawater, the NS1, NS2, D1, and D2 fluids contain 5.3, 25.2, 14.3, and 6.1 wt.% magmatic fluid, respectively.

Preservation of seawater Na:K:Mg ratios during mixing of magmatic fluid and seawater implies that the source of these elements is predominantly seawater and that chemical exchange of Na, K, and Mg with the crust is not occurring to a significant extent before or after mixing. This contrasts with previous interpretations that the elevated Mg in DESMOS fluids is derived from Mg-silicate dissolution (Gamo et al., 1997). The lack of chemical exchange involving Na, K, and Mg, however, should not be interpreted as an indication that fluid–rock reaction is not occurring in subsurface environments responsible for the formation of the acid-sulfate fluids. Indeed, measured concentrations of aqueous Fe, Al, and SiO_2 that approach several mmol/kg (Table 1) provide strong evidence for dissolution of Fe-, Al-, and Si-bearing mineral assemblages in response to the high acidity of these fluids. The conservative behavior of Na, K, and Mg may reflect the presence of a mineral assemblage depleted in Na, K, and Mg in upflow zones, or alternatively, equilibrium between the upflow zone minerals and the acid-sulfate fluids. Hydrothermal alteration of the oceanic crust in upflow zones typically occurs under fluid-dominated conditions resulting in an alteration rock chemistry and mineralogy dictated by fluid composition. Once equilibrium with a mixed fluid containing relative abundances of Na, K, and Mg inherited from seawater has been established, continued fluid flow at constant temperature and pressure will not result in net additional exchange of these elements. Mineral assemblages at DESMOS and the nearby PACMANUS hydrothermal systems, which are interpreted to have formed during advanced argillic alteration by acid-sulfate fluids, typically contain Na- and K-bearing alunite solid solutions, pyrophyllite, silica phases, anhydrite, and pyrite, but no Mg-bearing minerals (Gena et al., 2001; Lackschewitz et al., 2004; Paulick and Bach, 2006; Binns et al., 2007; Hrischeva et al., 2007). The presence of alunite solid solutions containing Na and K and the general absence of Mg-bearing minerals in acid-sulfate alteration assemblages at DESMOS and SuSu Knolls suggests that the apparent lack of Na and K exchange in the acid-sulfate fluids may reflect fluid–mineral equilibria with highly altered crust, while the lack of Mg exchange may reflect undersaturation of acid-sulfate fluids with respect to Mg-bearing minerals and their absence in upflow zones.

Limited Mn enrichment in the acid-sulfate fluids relative to dissolved Fe (Table 1) provides further support for interaction with highly altered rock in subsurface environments. Mn typically exhibits pH-dependent aqueous mobility similar to Fe during fluid-rock interaction (Seewald and Seyfried, 1990), but would be rapidly exhausted during hydrothermal alteration at high water/rock ratios due to its substantially lower concentration relative to Fe in basaltic and felsic crust of the Eastern Manus volcanic zone (Sinton et al., 2003). Limited Mn mobility is also consistent with the relatively minor enrichments of the mobile elements Li, Rb, and Cs that would also be rapidly depleted in highly altered rock under fluid-dominated conditions (high water/rock ratio). Thus, a fundamental difference between fluid-rock interaction responsible for the formation of acid-sulfate and black smoker fluids is that the former involves rocks that have been altered at very high integrated water/rock ratios, while the latter involves interaction with fresh crustal rocks at low water/rock ratios (Seyfried, 1987; Von Damm, 1995).

The influence of fluid–rock interaction on fluid composition during upflow can be assessed by examining the saturation state of venting fluids with mineral assemblages likely to exist beneath the seafloor. For this purpose, the fluid speciation and reaction path program EQ3NR/EQ6 version 8.0 (Wolery, 1992) was used to calculate the equilibrium distribution of aqueous species at the measured vent temperatures. The supporting thermodynamic database for these calculations was generated at 25 MPa using SUPCRT92 software (Johnson et al., 1992) that included thermodynamic data for minerals (Helgeson et al., 1978) and relevant aqueous inorganic species (Shock and Helgeson, 1988; Shock et al., 1989, 1997; Sverjensky et al., 1997). Thermodynamic properties for Al^{3+} and aqueous aluminum complexes in the SUPCRT92 database were updated with values from Tagirov and Schott (2001). During these calculations, redox equilibrium between aqueous sulfur species was suppressed so that that measured ΣH_2S and ΣSO_4 concentrations (25 °C) reflect *in situ* abundances. This assumption is supported by sluggish reaction kinetics for sulfide-sulfate equilibrium at 25 °C (Ohmoto and Lasaga, 1982) and the rapid cooling and processing

of samples after collection. Activity coefficients for charged aqueous species were calculated using the B-dot equation (Helgeson et al., 1981).

Results of equilibrium speciation calculations indicate that the acid-sulfate fluids are slightly undersaturated with respect to anhydrite (Fig. 3). In general, the degree of undersaturation decreases in the higher temperature fluids, consistent with the retrograde solubility of anhydrite (Holland and Malinin, 1979). Accordingly, there is a thermodynamic drive for anhydrite dissolution in subsurface environments by the relatively low temperature acid-sulfate fluids sampled at North Su and DESMOS. Fluid compositions that are below anhydrite saturation suggest that there is insufficient time for anhydrite dissolution to reach equilibrium or anhydrite is absent in some subsurface mixing environments.

The approach to near saturation as temperatures approach 215 °C in conjunction with decreasing anhydrite solubility at higher temperatures, suggests that the initial mixing of a ~1000 °C magmatic volatile phase with Ca-bearing seawater likely results in extensive precipitation of anhydrite and removal of Ca and SO_4 from solution in equimolar amounts. Observed Ca concentrations in acid-sulfate fluids at DESMOS and North Su that are above and below values expected for mixing of pristine seawater with a Ca-free magmatic fluid (Fig. 2) are consistent with both high temperature precipitation and low temperature dissolution.

The speciation calculations also indicate that the acid-sulfate fluids are undersaturated with respect to K-alunite and pyrophyllite (Fig. 3), the Al-bearing minerals likely to exist in regions of the crust extensively altered by highly-acidic and SO_4-rich fluids. As is the case for anhydrite, this creates a thermodynamic drive for dissolution of these minerals if present, and the release of K, Al, Si, and SO_4 to solution. The departure from equilibrium with

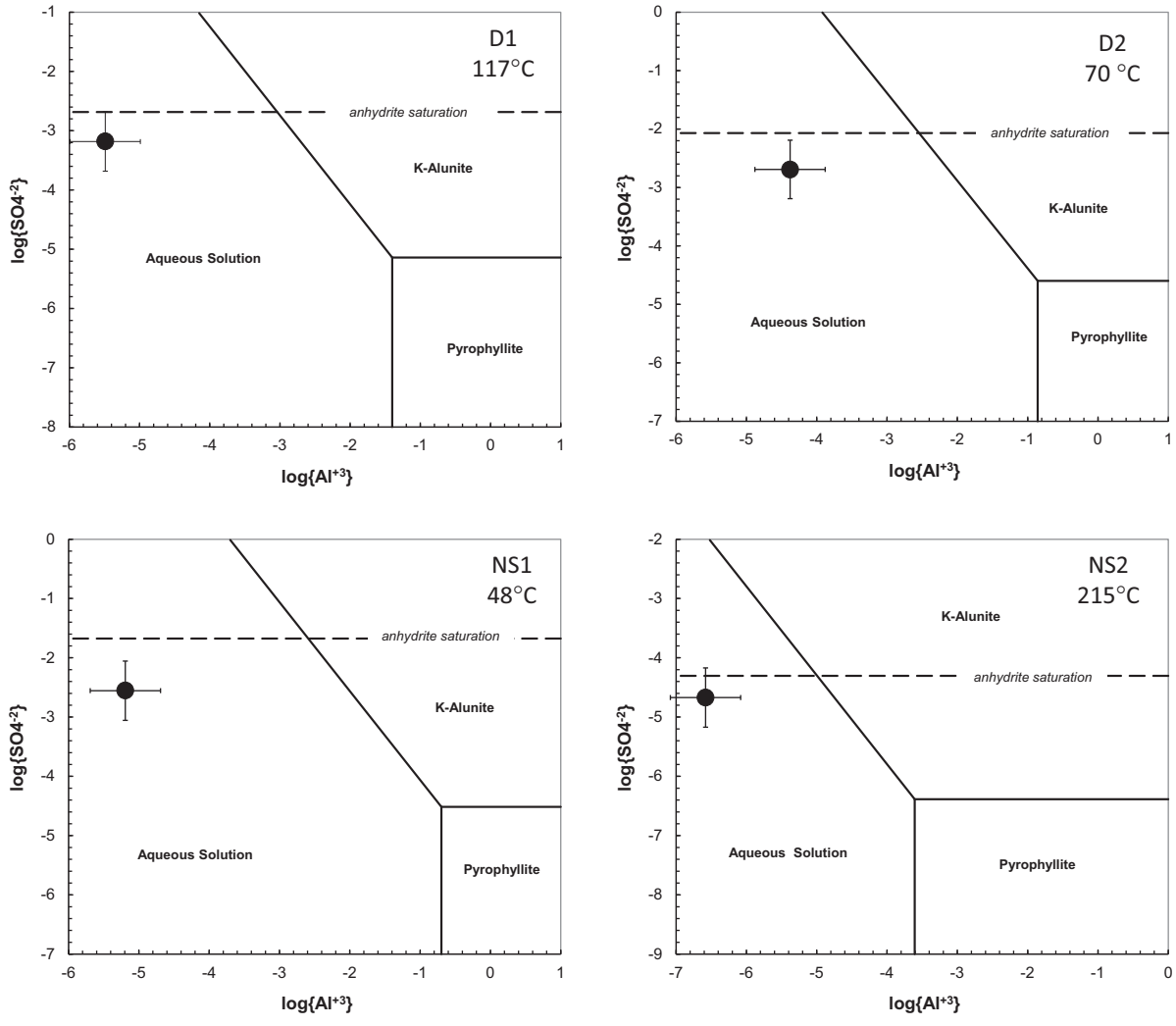

Fig. 3. Activity diagrams showing the stability of K-alunite and pyrophyllite in equilibrium with an aqueous phase for acid-sulfate vent fluids from the DESMOS and North Su vent areas at the indicated temperatures and 25 MPa. *In situ* activities of H^+, K^+, Ca^{2+}, SO_4^{2-}, and $SiO_{2(aq)}$ necessary for the construction of these diagrams were calculated using the computer program EQ3NR (Wolery, 1992) and the measured concentrations of aqueous species and temperatures at each vent. The error bars represent 0.5 log units.

these phases likely reflects decreasing reaction rates with decreasing temperature as the degree of subsurface mixing increases, and/or the possible absence of these minerals in the subsurface.

The composition of acid-sulfate fluids sampled at DESMOS and North Su in 2006 point to an absence of significant chemical exchange involving dissolved Na, K, and Mg during interaction with highly altered rocks in the upflow zone. This may not always be the case, however, since spatial and temporal variability in the release of magmatic volatiles, volcanic/magmatic activity, and crustal fracturing that may expose fresh or less altered rocks to ascending fluids. Reaction with less altered rocks likely results in some chemical exchange of Na, K, and Mg. Accordingly, the minor departure of Na, K, and Mg concentrations in the 1995 fluids (Gamo et al., 1997) relative to trends predicted for conservative mixing of a magmatic volatile and unmodified seawater for the DESMOS fluids in 1995 (Fig. 2) suggests the involvement of less altered rock during this earlier phase of hydrothermal activity. Similar minor enrichments of Na, K, and Mg were observed in acid-sulfate fluids at the Brothers intraoceanic arc volcano (de Ronde et al., 2011). The magnitude of these enrichments/depletions in Na, K, and Mg are small, however, suggesting that fresh rock is not abundantly present along fluid flow paths.

5.1.1. Magmatic volatiles

The composition of acid-sulfate fluids in the Eastern Manus Basin provides compelling evidence for a magmatic contribution of acidic volatile species to mixed fluids venting at the seafloor. In addition to abundant water and near zero Na, K, and Mg concentrations, fluids exsolving from silicic magma in near-arc environments such as DESMOS and North Su are also expected to contain abundant volatiles such as SO_2, HCl, HF, and CO_2 (Carroll and Webster, 1994; Yang and Scott, 2006). Degassing of SO_2 reflects a fundamental difference in the speciation of total S in back-arc/arc magmas relative to mid-ocean ridge settings, where total S in MORB melts is predominantly present as sulfide (Carroll and Rutherford, 1988; Carroll and Webster, 1994). Magmatic SO_2 strongly partitions into aqueous fluids exsolved from magmas (Scaillet and Pichavant, 2003) and undergoes disproportionation to produce reduced and oxidized sulfur species upon cooling according to the reactions:

$$4SO_{2(aq)} + 4H_2O = H_2S_{(aq)} + 3H_2SO_{4(aq)} \quad (1)$$

$$3SO_{2(aq)} + 2H_2O = S^0_{(s)} + 2H_2SO_{4(aq)} \quad (2)$$

While this process is generally assumed to occur below approximately 400 °C, the relative importance of reactions (1) and (2) is strongly dependent on temperature, redox state, pH, and total sulfur (i.e., initial SO_2) present (Iwasaki and Ozawa, 1960; Holland, 1965; Drummond, 1981; Kusakabe et al., 2000). As proposed by Gamo et al. (1997) for DESMOS fluids, this process provides an explanation for the elevated concentrations of ΣSO_4 and anomalously low $\delta^{34}S_{SO_4}$ values in acid-sulfate fluids relative to seawater (Table 1). Sulfuric acid produced by reactions (1) and (2), along with HCl and HF already present in a volatile magmatic phase, will greatly increase the acidity of the mixed fluid, thereby influencing rock alteration processes and its ability to transport sulfide mineral forming metals such as Fe, Cu, and Zn due to increases in their aqueous solubility.

If it is assumed that these magmatic fluids contain near-zero concentrations of Na, K, and Mg prior to mixing with seawater, the same approach used to determine the end-member composition of black smoker fluids (Von Damm et al., 1985) can be used to estimate the end-member composition of the magmatic fluid. Although extrapolation to zero-Na, -K, or -Mg could be used for this purpose, we have opted to use Mg because it is more likely to behave conservatively in acid-sulfate upflow zones due to the limited presence of Mg-bearing minerals in highly altered hydrothermal upflow zones in general (Alt and Bach, 2003) and the highly altered rocks associated with DESMOS venting (Gena et al., 2001), in particular. Results of these extrapolations (Fig. 4, Table 2) yield end-member magmatic fluid concentrations for ΣSO_4 and residual SO_2 that vary from 205 to 710 mmol/kg and 58 to 131 mmol/kg, respectively. Collectively, these concentrations suggest that the initial SO_2 content of the magmatic fluid end-member prior to disproportionation ranges from 0.39 to 1.2 mol/kg if it is assumed that reaction (2) is the primary pathway for SO_2 disproportionation (Table 2). The lack of substantial dissolved ΣH_2S, which in some cases was below detection (Table 2), and the abundance of particulate elemental sulfur (S^0) either as 'white smoke' or in molten deposits surrounding the vents, implicate reaction (2) as the dominant mechanism of disproportionation in both the DESMOS and North Su acid-sulfate fluids in 2006.

The speciation of sulfur during disproportionation is strongly influenced by *in situ* pH, dissolved H_2, and temperature (Fig. 5). A likely explanation for the predominance of reaction (2) at DESMOS and North Su is the high initial SO_2 content of the magmatic fluids involved. At total S concentrations similar to the initial SO_2 content of the D1 vent (1.2 mol/kg), disproportionation between 300 and 400 °C occurs primarily via reaction (2) and does not produce H_2S due to the large stability field of elemental S^0 (Fig. 5a and b). Below 300 °C, SO_2 is increasingly unstable. The presence of minor quantities of ΣH_2S and abundant elemental S^0 (white smoke) in vents D2 and NS1, in contrast, is likely a result of the lower initial SO_2 in these vents relative to D1 and NS2. Under such conditions, it is possible for disproportionation to initially occur by reaction (1) at higher temperatures, producing H_2S (Fig. 5c), but as magmatic fluids cool further during mixing, reaction (2) becomes increasingly more important (Fig. 5d). The occurrence of both mechanisms as a function of total S and temperature would also account for the presence of H_2S as well as particulate S^0 and HSO_4^- in these fluids, as opposed to only the latter two products of disproportionation in vents D1 and NS2 (Table 2).

The low H_2 contents of the acid-sulfate fluids (1.7–22 μmol/L) relative to black smoker fluids from back-arc and mid-ocean ridge environments (Charlou et al., 2000, 2002; Lilley et al., 2003; Seewald et al., 2003; Reeves

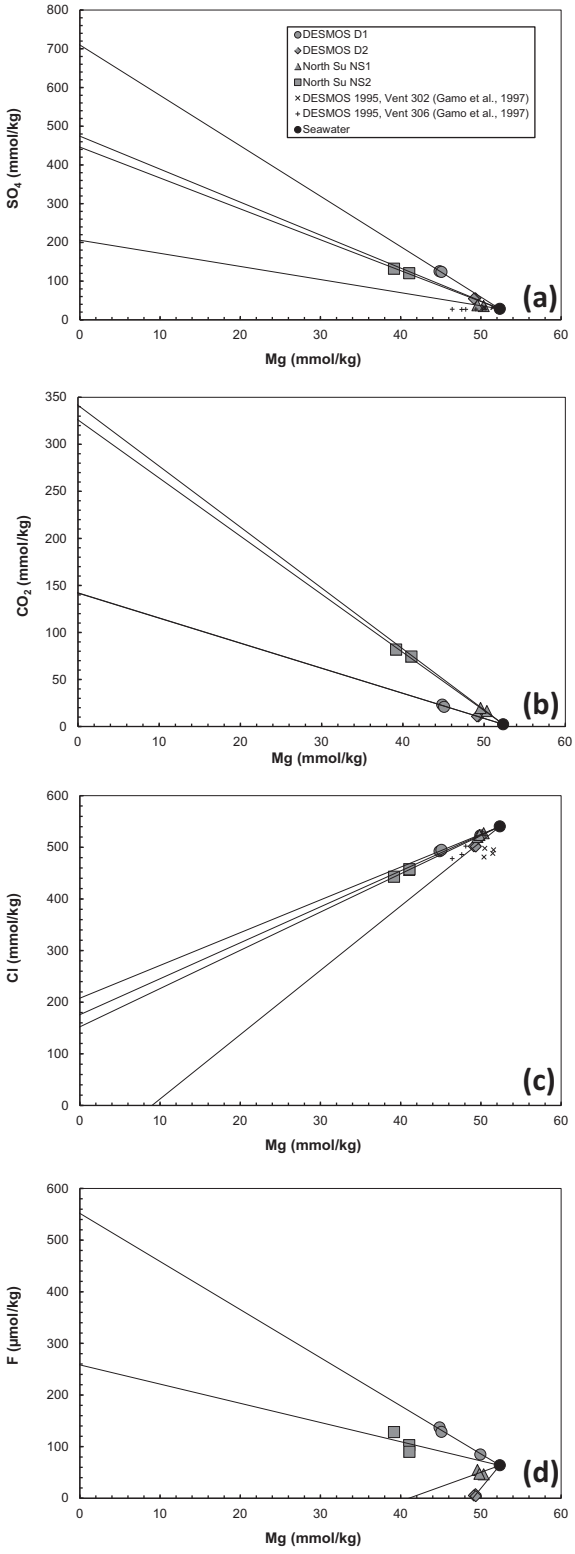

Fig. 4. Concentrations of selected aqueous species versus aqueous Mg in acid-sulfate vent fluids collected from the DESMOS and North Su vent areas in 2006.

et al., 2011; Pester et al., 2012) are also broadly consistent with the range of redox conditions expected for disproportionation under scenarios similar to those illustrated in Fig. 5. It is likely that the speciation of magmatic sulfur plays an important role in regulating dissolved H_2 concentrations in these fluids. In subaerial volcanic systems, magmatic H_2 and/or hydrothermal alteration of unaltered Fe-bearing rocks in volcanic vent conduits can contribute H_2 to hydrothermal fluids that may react with SO_2 to form H_2S under high temperature conditions. Consumption of H_2 by this mechanism may lead to redox buffering of the fluids by the SO_2/H_2S couple (Taylor, 1986; Giggenbach, 1997). However, the lack of substantial H_2 or ΣH_2S in the fluids and the highly altered nature of mineral assemblages in the upflow zones at DESMOS and North Su suggest that disproportionation alone dominates the fate of SO_2 and fluid/rock reactions in hydrologic conduits have a minimal influence on the redox state of venting fluids at these locations.

Owing to the coexistence of relatively high ΣSO_4 concentrations with aqueous Ca in the DESMOS and North Su fluids at elevated temperatures, it is possible that anhydrite precipitation may have influenced the measured ΣSO_4 concentrations which, in turn, would introduce systematic errors to the estimation of the endmember magmatic values. Measured Ca concentrations in some fluids, however, are above values expected for mixing of seawater and a magmatic fluid (Fig. 2), which by analogy to Na, K, and Mg, would be expected to contain near zero-Ca. Concentrations of Ca in 2006 that are above values expected for conservative mixing suggest previously deposited anhydrite may be dissolving in subsurface environments, contributing both Ca and SO_4 to solution. Reported concentrations of Ca in 1995 (Gamo et al., 1997) that are below values expected for conservative mixing (Fig. 2) suggest an earlier period of anhydrite precipitation. Anhydrite is a common subsurface mineral at SuSu Knolls and would likely dissolve or precipitate to maintain equilibrium with the fluid as temporal and spatial variations in temperature and fluid composition change the saturation state of ascending fluids. Although addition of SO_4 by anhydrite dissolution would result in end-member ΣSO_4 concentrations that are systematically too high, the relatively minor enrichment of Ca above the dilution trend for seawater (Fig. 2) indicates that the effect on extrapolated ΣSO_4 values is relatively minor.

Other magmatic volatile species also show large enrichments in the acid-sulfate fluids. Estimated end-member ΣCO_2 concentrations range from 142 to 341 mmol/kg (Fig. 4b, Table 2), values that are well below CO_2 solubility at seafloor pressures, consistent with the absence of liquid CO_2 associated with the white smoker vents. The extrapolated endmember Cl concentration in the NS1, NS2, and D1 fluids vary from 152 to 209 mmol/kg. Extrapolation of the measured Cl abundance in the D2 fluid to zero Mg results in an apparent negative end-member concentration (Fig. 4c) that may reflect analytical uncertainty and large extrapolation errors due to the near-seawater Mg concentration for this fluid, but it may also indicate non-conservative behavior of Mg in the upflow zone. That the measured Na and K concentrations in the D2 fluid are also slightly below values predicted for conservative

Table 2
Calculated concentrations* and isotopic composition of selected species in end-member magmatic volatile phases at the DESMOS and North Su vent fields.

Field Vent	Cl mm	F μm	SO_4 mm	$\delta^{34}S_{SO_4(mag)}$ † ‰	SO_2 mm	SO_{2init} ‡ mm	CO_2 mm	$\delta^{13}C_{CO_2}$ ‰	$\delta^{18}O_{H_2O}$ ‰	δD_{H_2O} ‰
DESMOS										
D1	209	552	710	7.0	131	1196	142	−3.4	6.5	-31
D2	nd	nd	474	13.9	103	814	142	−4.6	nd	nd
North Su										
NS1	176	nd	205	14.1	80	388	341	−2.8	nd	nd
NS2	152	258	446	nd	58	727	326	−2.9	8.3	-26

* mm = mmol/kg fluid, μm = μmol/kg fluid, nd = not determined.
† Isotopic composition of SO_4 derived from disproportionation of magmatic SO_2 prior to seawater mixing.
‡ Concentration of SO_2 in end-member magmatic fluid prior to disproportionation.

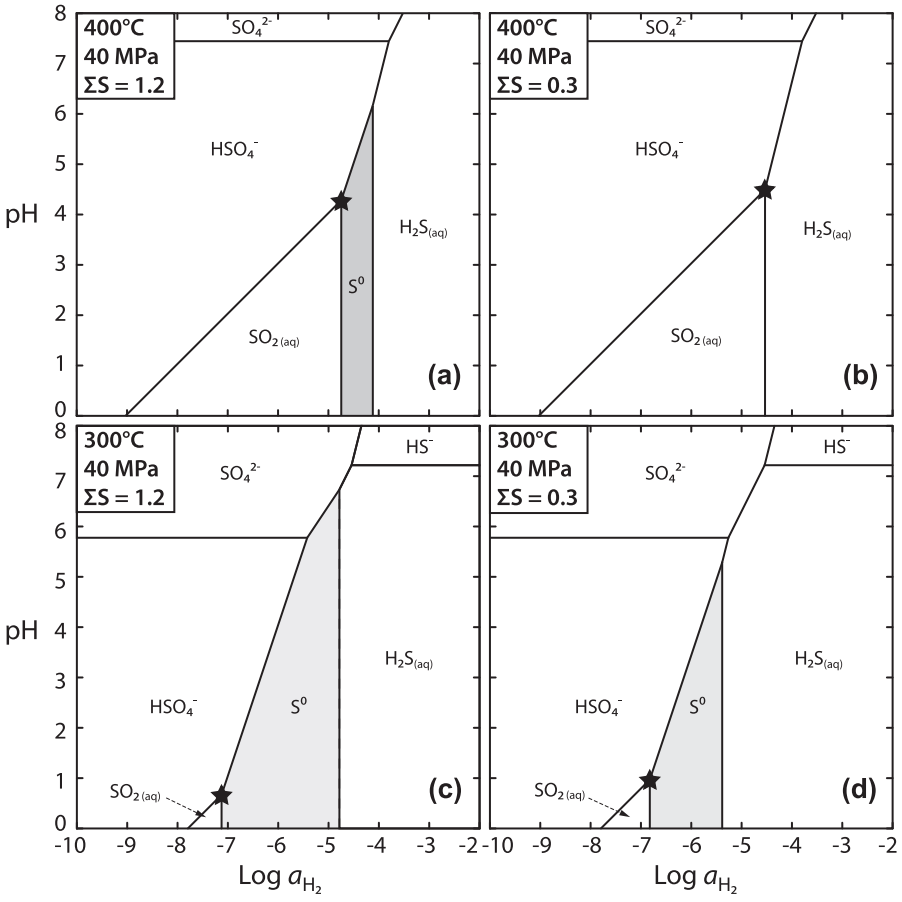

Fig. 5. Activity–activity diagrams in the system SO_2–H_2O at 400 °C (A) and 300 °C (B) for a total S concentration (ΣS) of 1.2 mol/kg H_2O as a function of pH and dissolved H_2 activity (a_{H_2}). Similar diagrams at 400 °C (C) and 300 °C (D) are shown for a ΣS concentration 0.3 mol/kg H_2O. All diagrams are constructed for a pressure of 40 MPa. Activity coefficients of unity have been assumed for all species included in these diagrams. The star represents the triple point where $SO_{2(aq)}$, HSO_4^- and either elemental S^0 or $H_2S_{(aq)}$ are in equilibrium. These diagrams were generated using thermodynamic data from Helgeson et al. (1978) and Shock et al. (1989, 1997).

mixing (Fig. 2) suggests that a minor amount of Mg (<2 mmol/kg) may have been added to the fluid before and/or after mixing.

Based on the compositions of olivine-hosted melt inclusions from Pual Ridge that contain F (Yang and Scott, 2002), and the substantial F enrichments in PACMANUS hydrothermal fluids (Reeves et al., 2011), a contribution of F from a magmatic fluid is also to be expected at DESMOS and North Su. Extrapolation of measured F concentrations to zero-Mg, however, yields both negative and positive values (Fig. 4d). Apparent negative values are not possible and indicate removal of F from solution during

upflow. Laboratory experiments have demonstrated rapid F-fixation during heating of seawater at 150–250 °C that was best accounted for by substitution of F for hydroxyl groups in hydrous phases (Seyfried and Ding, 1995). In contrast, at temperatures ⩾250 °C, F solubility was observed to increase due to enhanced stability of the aqueous HF° complex (Seyfried and Ding, 1995). The primary magmatic F contribution in acid-sulfate fluids is likely obfuscated by both enrichment and depletion owing to fixation in or mobilization from abundant hydroxyl-bearing minerals such as alunite and pyrophyllite over the broad range of temperatures in subsurface mixing zones at DESMOS and SuSu Knolls. Nonetheless, the maximum end-member F concentration calculated for the acid-sulfate fluids is 552 μmol/kg, which is approximately two orders of magnitude lower than the other volatile magmatic species, suggesting that it is a relatively minor component of the magmatic fluid. Collectively, the composition of acid-sulfate fluids indicates an end-member magmatic fluid phase where $H_2O > SO_2 > CO_2 \approx Cl > F$ defines the relative abundance of dominant constituents, and generally resembles the composition of magmatic fluids inferred to have exsolved from highly fractionated felsic magmas at PACMANUS (Yang and Scott, 2002; Reeves et al., 2011).

The composition of end-member magmatic fluids can also be used to assess the extent that acidic volatiles influence the measured pH of acid-sulfate fluids at DESMOS and North Su. The amounts of acidity added to the vent fluids can be calculated by assuming conservative mixing of the magmatic end-member fluid and seawater assuming that a mole of HCl and a mole of H_2SO_4 contribute one and two equivalents of acidity, respectively. Calculating the pH (25 °C) of the mixed fluids requires accounting for the speciation of aqueous sulfate species because HSO_4^- is a weak acid ($pK_a = 2.0$ at 25 °C and 100 kPa) and seawater and magmatic-derived ΣSO_4 exist as both HSO_4^- and SO_4^{2-} at the pH of the mixed fluids. Using activity coefficients for charged species calculated for a seawater salinity fluid, estimated pH (25 °C) values show excellent agreement with values measured for the fluids sampled as DESMOS and North Su (Fig. 6). The small positive departure of the estimated pH relative to the measured value for the D2 fluid likely reflects the absence of a reliable estimate for the abundance of HCl in the magmatic end-member that would contribute additional acidity. The similarity of measured and estimated pH (25 °C) provides additional evidence confirming magmatic volatiles as the dominant source of acidity in acid-sulfate fluids at DESMOS and North Su. Moreover, the conservative behavior of acidity during upflow and mixing with seawater indicates that pH is not modified by extensive fluid–rock interactions in the subsurface, consistent with the lack of large enrichments in the abundance of the major cations Na, K, and Mg and preservation of seawater abundance ratios.

5.1.2. Thermal constraints

Further confirmation that magmatic fluid-seawater mixing is generating acid-sulfate fluids is provided by their measured temperatures. The observation that replicate fluid samples from a given vent yield reproducible Mg

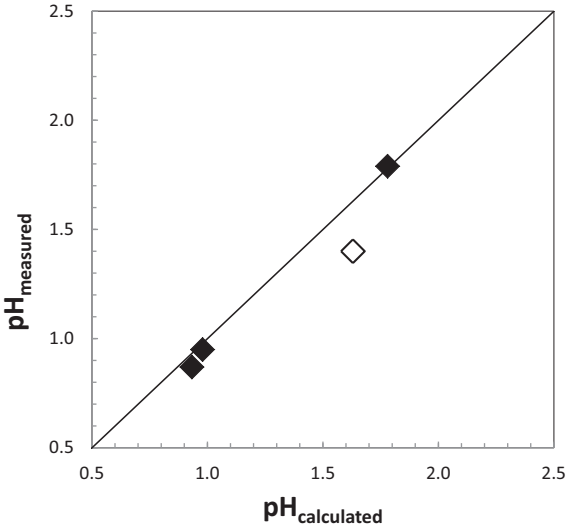

Fig. 6. Calculated pH (25 °C) versus measured pH (25 °C) for acid-sulfate fluids from the DESMOS and North Su vent fields. The positive deviation of the D2 vent (open symbol) likely reflects the absence of data for the concentration of HCl in the end-member magmatic fluid that represents a source of acidity in these fluids.

concentrations indicates that subsurface mixing is occurring prior to venting. This allows the Mg concentrations of the fluids exiting the seafloor to be used together with the maximum measured vent temperatures to estimate the end-member temperature of the magmatic fluid. For the purpose of these calculations, enthalpy values for pure water from the NIST Chemistry WebBook (Linstrom and Mallard, 2014) were employed along with the assumption that enthalpy is conserved during mixing. Although the use of enthalpy values for pure water introduces a small amount of error into these calculations, the absence of an equation of state for variable composition and salinity fluids over the entire temperature range of interest precludes a more rigorous approach. Heat capacity data for seawater salinity fluids at a given temperature and pressure (Bischoff and Rosenbauer, 1985) are lower than that of pure water resulting in a maximum error of approximately 20 °C for the calculated temperatures during mixing (Fig. 7). Examination of Fig. 7 reveals estimated end-member magmatic temperatures that vary from 600 to 1000 °C, a range that is consistent with likely temperatures for silicic magmas existing in this region of the Manus Basin (Sinton et al., 2003). This range is comparable to that estimated for magmas associated with terrestrial fumaroles in subduction-related settings, (e.g., Giggenbach, 1992; Hedenquist et al., 1994; Hedenquist and Lowenstern, 1994). The ability of the above approach to predict magmatic temperatures along with the strong correlation between measured temperature and Mg that passes through 2 °C, suggest that conductive heating of seawater is not occurring to a significant extent prior to mixing of these fluids.

In contrast to black-smoker fluids that require conductive heating of seawater in the vicinity of a crustal magma chamber or hot rock prior to convective transport to the

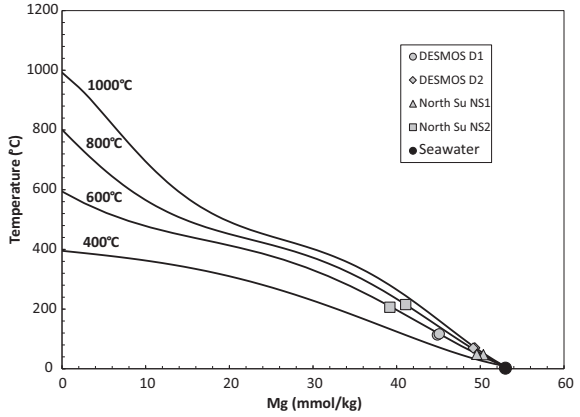

Fig. 7. Measured temperatures versus aqueous Mg for acid-sulfate vent fluids collected from the DESMOS and North Su vent areas in 2006. The solid lines show predicted temperatures during mixing of Mg-free high temperature magmatic fluids (temperatures indicated) with a Mg-bearing (53 mmol/kg) 2 °C fluid. See text for details relevant to the construction of this figure.

seafloor (Alt, 1995), the primary mechanism for heat transport in areas of acid-sulfate fluid venting is by direct advection of magmatic volatiles from crustal magma chambers. Because volatiles contain a small fraction of the heat available within a magma body, the amount of heat that can be removed by this mechanism is substantially less than during convective circulation of seawater-derived hydrothermal fluids that can access the entire heat inventory within a magma chamber via thermal conduction. This has important implications for the cooling of oceanic crust since venting of acid-sulfate fluids is unlikely to play a significant role in the cooling of sub-seafloor magma chambers or newly erupted lavas.

The chemical composition and heat content of acid-sulfate fluids at DESMOS and North Su can be accounted for by mixing of hot magmatic volatiles and cold unmodified seawater followed by chemical interaction with highly altered rocks within hydrothermal upflow zones. There are significant differences between this model and that postulated for the formation of black-smoker type fluids in back-arc and arc environments that have implications for chemical exchange and subsurface alteration processes. Perhaps most important, is that the formation of acid-sulfate fluids at DESMOS involves the mixing of two endmember fluids, magmatic volatiles and cold seawater, whereas formation of nearby black-smoker fluids (e.g., at PACMANUS, or at the summit of North Su) typically contain variable contributions from three endmember fluids; an evolved seawater-derived hydrothermal fluid that has experienced extensive interaction with unaltered rocks at low water/rock ratio, a magmatic volatile-rich fluid, and unmodified cold seawater (de Ronde et al., 2011; Mottl et al., 2011; Reeves et al., 2011). Black smoker fluids are characterized by higher pH (25 °C) relative to acid-sulfate fluids and, prior to mixing with cold-seawater, the near quantitative removal of aqueous Mg and ΣSO_4 (de Ronde et al., 2011; Mottl et al., 2011; Reeves et al., 2011). For black-smoker fluids that contain a significant magmatic component, the higher pH and absence of aqueous ΣSO_4 derived from magmatic SO_2 disproportionation (reactions 1 and 2) requires a mechanism to titrate acidity and remove ΣSO_4 from solution following the addition of acidic magmatic volatiles. Exchange of H^+ for cations such as Na^+, K^+, Ca^{2+}, and Fe^{2+} during interaction with relatively fresh rock represents a viable mechanism to titrate acidity and release rock-derived Ca necessary to remove SO_4 as anhydrite ($CaSO_4$) (Seyfried, 1987). Continuous access to fresh rock by black smoker fluids following the addition of magmatic volatiles likely reflects the progression of a cracking front to adjacent the magma chamber as rocks solidify and contract in response to efficient heat extraction by convecting hydrothermal fluids (Lister, 1974, 1983). Thus, the apparent paucity of fresh rock encountered during the formation of acid-sulfate fluids may reflect the absence of thermal convection that is responsible for the heat extraction necessary to induce thermal cracking during the cooling of crustal rocks.

5.1.3. Isotopic constraints

The origin of acidic and sulfate-rich fluids venting at DESMOS and North Su can be further assessed by examining the abundance of stable hydrogen and oxygen isotopes in water, carbon isotopes in dissolved ΣCO_2, and sulfur isotopes in ΣSO_4. The measured hydrogen isotopic composition of H_2O in these fluids varies from $-1‰$ to $-8‰$ and the oxygen isotopic composition from $0.2‰$ to $2.2‰$; values consistent with the isotopic composition of fluids sampled at DESMOS in 1995 by Gamo et al. (1997). Gena et al. (2006) calculated a similar isotopic composition for the hydrothermal fluids that produced kaolinite-bearing alteration assemblages at DESMOS. The substantial D depletions that characterize the DESMOS and North Su fluids are in marked contrast to the D enrichments observed in typical basalt-hosted black-smoker fluids that result from hydration reactions during fluid–rock interaction at elevated temperatures and pressures (Bowers and Taylor, 1985; Bowers, 1989; Shanks et al., 1995; Shanks, 2001). Although negative δD values in the acid-sulfate fluids could be produced by fluid interaction with nearby hemipelagic sediments at DESMOS and North Su (Shanks, 2001), such interaction would likely be accompanied by the production of thermogenic CH_4 from sedimentary organic matter (Seewald et al., 1990, 1994). The low abundance of CH_4 in these fluids (Table 1) indicates that extensive interaction with sediments has not occurred. It is possible to generate negative δD values for low salinity hydrothermal fluids during some open system scenarios of subcritical phase separation (Berndt et al., 1996), but these involve unusually extreme distillation of vapor phases, or phase separation of pre-existing brines. Given the other compositional attributes of these fluids, the negative δD values for acid-sulfate and black-smoker fluids in the Eastern Manus Basin can be attributed to the subsurface addition of magmatic volatiles and subsequent mixing with seawater (Gamo et al., 1997; Gena et al., 2006; Reeves et al., 2011).

If a model involving the mixing of a Mg-free aqueous magmatic fluid and seawater as described above is

embraced for the origin of acid-sulfate fluids at DESMOS and North Su, the isotopic composition of the magmatic end-member can be calculated by linearly extrapolating the measured isotopic compositions to zero Mg. Although this can be done for all the sampled fluids, large extrapolation errors result for vent fluids that contain near seawater Mg concentrations due to the magnitude of analytical uncertainties associated with the hydrogen isotopic measurements. Accordingly, magmatic end-members were not calculated for the D2 and NS1 vents, which had compositions close to seawater. Extrapolations of the measured isotopic compositions for the D1 and NS2 vents to zero Mg yields an end-member magmatic volatile characterized by δD values of −31‰ and -26‰ and $\delta^{18}O$ values of 6.5‰ and 8.3‰, respectively. Examination of Fig. 8 reveals that these values are far more D-enriched than typical juvenile mantle derived magmatic H_2O (Taylor, 1979b; Ohmoto, 1986).While isotope fractionation effects during degassing from silicic magma could substantially enrich the D content of exsolved juvenile H_2O (e.g., Holloway and Blank, 1994), the values calculated above are similar to estimated compositions of waters degassed from arc magmas argued to have been compositionally modified by 'devolved seawater' from the subducting slab (Giggenbach, 1992; Hedenquist and Lowenstern, 1994; Shaw et al., 2008). This agreement is noteworthy since the isotopic compositions of magmatic fluid calculated here are extrapolated from near seawater compositions, whereas the devolved seawater composition discussed by Giggenbach (1992) were extrapolated from compositions heavily diluted by meteoric waters characterized by much lower δD values.

The acid-sulfate vents at DESMOS and North Su suggest the widespread occurrence of such isotopic compositions in subduction-related settings, and provide

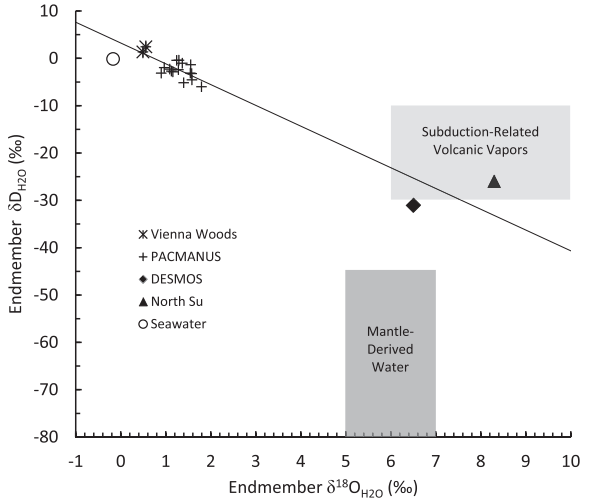

Fig. 8. End-member δD_{H_2O} and $\delta^{18}O_{H_2O}$ values for vent fluids from the Manus Basin. Values for the Vienna Woods and PACMANUS vent fields are from Reeves et al. (2011). The shaded regions show the range of values for mantle-derived water (Taylor, 1979b; Ohmoto, 1986) and subduction related volcanic vapors (Giggenbach, 1992; Hedenquist and Lowenstern, 1994). The solid line represents a linear regression of the data from the PACMANUS and Vienna Woods hydrothermal fields.

compelling evidence for a contribution of slab-derived H_2O to melts generated in the back-arc environment of the Eastern Manus Basin. This is consistent with numerous geochemical proxies (e.g., higher Ba/Nb and Cl/Nb ratios in dredged lavas) that indicate substantial subduction-related inputs to magmas in the Eastern Manus volcanic zone (Kamenetsky et al., 2001; Sinton et al., 2003; Sun et al., 2004; Pearce and Stern, 2006; Park et al., 2010). In addition to hydrated basaltic crust, sediments overlaying the Solomon Sea plate undergoing subduction beneath the New Britain arc are characterized by indurated mudrocks (claystones and calcareous mudstones) and pelagic limestones (Crook, 1987) that would contribute water compositionally similar to the estimates of Giggenbach (1992). This conclusion differs from the model proposed previously for the formation of DESMOS acid-sulfate fluids that involves addition of juvenile mantle-derived H_2O characterized by the δD values of −40‰ to −80‰ (Gamo et al., 1997; Gena et al., 2006).

Additional evidence documenting a contribution of volatiles from the subducting slab underlying the Eastern Manus Basin volcanic zone is provided by the carbon isotopic compositions of ΣCO_2 in DESMOS and North Su acid-sulfate fluids that vary from −2.8‰ to −4.6‰ when corrected for the contribution of admixed seawater (Table 2). This range of values is enriched in ^{13}C relative to ΣCO_2 observed in basalt-hosted mid-ocean ridge hydrothermal fluids with $\delta^{13}C$ values that typically vary from −4‰ to −9‰ (Kelley et al., 2004). The relatively high $\delta^{13}C_{CO_2}$ values suggest a contribution of ^{13}C-enriched carbon to magmatic fluids from slab-derived carbonates (Alt and Teagle, 1999; Coltice et al., 2004). Although fluid interaction with nearby hemipelagic sediments at DESMOS and North Su could result in the dissolution of ^{13}C-enriched marine carbonate and an increase in the $\delta^{13}C_{CO_2}$ values of acid-sulfate fluids, as discussed above, low values of CH_4 in DESMOS and North Su acid-sulfate fluids indicate that interaction with sediments is not occurring to a significant extent. The range of $\delta^{13}C_{CO_2}$ values in the acid-sulfate fluids at DESMOS and North Su are similar to the those for ΣCO_2 in vent fluids from the nearby PACMANUS vent field (−2.3‰ to −4.1‰), but are enriched relative to ΣCO_2 from the Vienna Woods vent field (−5.2‰ to −5.7‰), approximately 170 km to the west (Reeves et al., 2011). Elevated ^{13}C contents in the eastern most vent fields likely reflects an increased contribution of slab-derived CO_2 as the New Britain arc is approached (Fig. 1). Values of $\delta^{13}C$ for magmatic CO_2 venting at Rabaul Caldera located at the New Britain Arc vary from −2‰ to −5‰ (Pérez et al., 1996), almost identical to the range observed here for DESMOS and North Su. A similar trend has been observed in Lau Basin where the influence of the subducting slab on the composition of ridge-crest vent fluids increases systematically from north to south as the back-arc spreading center approaches the Tofua arc (Proskurowski et al., 2007; Mottl et al., 2011).

The observed S isotope fractionation between dissolved ΣSO_4 and particulate elemental S^0 collected in the IGT samplers is consistent with SO_2 disproportionation via reaction (2) at temperatures expected for this reaction (Fig. 5).

Measured $\delta^{34}S_{SO_4}$ values undoubtedly contain a contribution of seawater-derived ΣSO_4 and must be corrected to estimate the $\delta^{34}S_{SO_4}$ value of the magmatic SO_2-derived fraction of ΣSO_4. Using only fluids that show minimal deviations in measured Ca (D1, NS1 and NS2) and are therefore not substantially affected by anhydrite dissolution or precipitation, the following isotope mass balance for $\delta^{34}S_{SO_4}$ values of measured ΣSO_4 can be assumed:

$$\delta^{34}S_{SO_4(meas)} = \delta^{34}S_{SO_4(sw)} * F_{SO_4(sw)} + \delta^{34}S_{SO_4(mag)} * (1 - F_{SO_4(sw)}) \quad (3)$$

where $F_{SO_4(sw)}$ is the fraction of the measured ΣSO_4 concentration assumed to be derived from seawater ΣSO_4 and $\delta^{34}S_{SO_4(meas)}$, $\delta^{34}S_{SO_4(sw)}$, and $\delta^{34}S_{SO_4(mag)}$ refer to the sulfur isotopic composition of measured, seawater-, and magmatic-derived ΣSO_4, respectively. Given the likely conservative behavior of admixed seawater Mg and ΣSO_4 following disproportionation discussed previously, it is assumed that $F_{SO_4(sw)}$ is directly proportional to the measured Mg concentration:

$$F_{SO_4(sw)} = ([Mg]_{meas}/[Mg]_{sw}) * ([\Sigma SO_4]_{sw}/[\Sigma SO_4]_{meas}) \quad (4)$$

where square brackets refer to the aqueous concentration of the species indicated. Values of $\delta^{34}S_{SO_4(mag)}$ calculated from Eq. (3) range from +7.0‰ to +14.1‰ at DESMOS and North Su (Table 2). While disproportionation may be happening over a range of temperatures during fluid ascent and mixing, $\delta^{34}S$ values of particulate elemental S^0 found in the fluid samplers (Table 1) provide the closest possible estimate of the isotopic composition of S^0 likely produced in association with magmatic SO_2-derived ΣSO_4 in the acid-sulfate fluids. The difference between $\delta^{34}S$ values for SO_2-derived ΣSO_4 and particulate S^0 at both DESMOS and North Su ($\Delta^{34}S_{SO_4 \leftrightarrow S^0}$) varies from 12.2‰ to 17.7‰. Based on equilibrium fractionation factors determined experimentally by Kusakabe et al. (2000) from 150 to 326 °C, and the isotopic composition of SO_2-derived ΣSO_4 and particulate S^0, equilibrium temperatures in excess of 400 °C are estimated, considerably higher than measured seafloor vent temperatures.

5.2. Comparison with previous studies

Comparison of the fluid chemistry presented here for the DESMOS vent area with the composition of DESMOS fluids in 1995 and 1998 (Gamo et al., 1997; Gena et al., 2006) reveals both similarities and differences. In general, the compositions of the 1995 fluids are consistent with trends that result from the dilution of seawater by a water-rich magmatic fluid (Figs. 2 and 4). Fluids collected in 2006, however, contain lower fractions of admixed seawater, allowing us to better resolve the composition of the magmatic end-members. The reason for this difference is not clear, but could reflect differences in the sampling devices used for fluid collection or temporal variability in subsurface hydrology. DESMOS fluids venting at the seafloor in 2006 contain substantially greater Al concentrations than were observed in 1995. The high levels of dissolved Al suggest that fluids of this type may be responsible for the formation of Al-rich plumes observed in the water column 200 m above the seafloor in 1990 (Gamo et al., 1993). Measured aqueous Al abundances and temperatures at DESMOS in 2006 suggest that dilution factors of 2000–4000 would be required to account for the observed water-column temperature anomaly of 0.03 °C and 320–1000 to account for the maximum 1.5 μmol/kg Al anomaly (Gamo et al., 1993). Moreover, Values of Al/Mn in the 2006 DESMOS vent fluids vary from 8 to 37, a range of values that shows significant overlap with the range of Al/Mn in the 1990 plume that vary from 10 to 18 (Gamo et al., 1993).

Maximum measured temperatures at the DESMOS area of venting have remained relatively constant from 88 to 120 °C in 1995 (Gamo et al., 1997) to 70 to 117 °C in 2006. However, temporal changes in dissolved S species are apparent that likely reflect variability in the extent of magmatic SO_2 degassing and subsequent disproportionation reactions. In particular, the measured ΣH_2S:ΣSO_4 ratio has systematically decreased in fluids collected on three different sampling occasions during this period. The highest ΣH_2S concentration of 8.1 mmol/kg was measured in 1995 (Gamo et al., 1997), but decreased to 2.8 mmol/kg in 1998 (Gena et al., 2006), and to <0.5 mmol/kg in 2006. Maximum measured ΣSO_4 concentrations, in contrast, increased from 32.8 mmol/kg in 1995 (Gamo et al., 1997) to 51.6 mmol/kg in 1998 (Gena et al., 2006) to 125 mmol/kg in 2006. These trends cannot be explained by different seawater:magmatic fluid mixing ratios, given the similarities in the estimated extent of dilution between 1995 and 2006 based on Mg concentrations and measured temperatures. While it is not possible to assess the fraction of residual SO_2 that was present in the 1995 fluids collected by Gamo et al. (1997), the measured ΣH_2S and ΣSO_4 data combined suggest a magmatic SO_2 contribution of approximately 0.3 mol/kg. This is substantially less than the 1.2 mol/kg calculated in 2006, assuming negligible residual SO_2 in the 1995 fluids. The 2006 increase must reflect an increased abundance in the magmatic end-member since seawater:magmatic fluid ratios appear to have remained constant. An increase in the total S content of the magmatic fluid venting at DESMOS that is accompanied by a marked decrease in the abundance of ΣH_2S from 1995 to 2006 is consistent with a shift from disproportionation proceeding via both reactions (1) and (2) in 1995 and 1998, to disproportionation occurring exclusively via reaction (2) in 2006 (Fig. 5). Increased acidity that would accompany increases in the contribution of magmatic SO_2 to venting fluids may also account for the enhanced Al dissolution and lower pH of fluids in 2006. Temporal changes in SO_2 fluxes on yearly to decadal timescales at DESMOS are similar to the variations reported for subaerial volcanic systems (e.g., Caltabiano et al., 1994; Kusakabe et al., 2000) and likely reflect changes in subsurface magmatic activity.

Further evidence pointing to an increase in the flux of magmatic SO_2 instead of temperature as the likely cause for changes in the DESMOS acid-sulfate fluids between 1995 and 2006 includes the broad similarity in temperatures of SO_2 disproportionation estimated from both datasets. Based on the S isotope fractionation between dissolved ΣH_2S and ΣSO_4 ($\Delta^{34}S_{SO_4 \leftrightarrow H_2S}$) at DESMOS in 1995,

Gamo et al. (1997) argued that disproportionation was occurring via reaction (1) at a temperature of ~250 °C, much lower than temperature estimates based on the 2006 compositions. However, the interpretation of Gamo et al. (1997) does not fully correct for the contribution of seawater-derived ΣSO_4 and therefore overestimates the magmatic $\delta^{34}S_{SO_4}$ value. The reported isotopic and chemical compositions for the 88 °C fluid collected in 1995 (samples 302-1 and 302-2 from Gamo et al., 1997), Eqs. (3) and (4), and the temperature dependency for equilibrium SO_4–H_2S isotopic fractionation determined by Ohmoto and Lasaga (1982) yield $\Delta^{34}S_{SO_4 \leftrightarrow H_2S}$ values of 16.3‰ and 18.0‰ that suggest much higher temperatures from 335 to 368 °C in 1995. Isotopic data for elemental S^0 collected in 1995 immediately adjacent to the 302-1 and 302-2 samples during the same dive (Gena et al., 2006) allows estimation of temperature based on SO_4–S^0 fractionation. Using the magmatic $\delta^{34}S_{SO_4}$ values calculated for 1995, estimated $\Delta^{34}S_{SO_4 \leftrightarrow S^0}$ values range from 17.3‰ to 20.0‰ and yield ΣSO_4–S^0 equilibrium temperatures >350 °C. Collectively, these observations suggest the temperature range in which disproportionation likely occurred in 1995 is indistinguishable from that of the 2006 fluids, and suggest that temperature is not the dominant factor responsible for the shift in disproportionation mechanisms.

Direct addition of magmatic volatiles to highly acidic, sulfate-rich vent fluids has also been reported for hydrothermal activity during active eruption of the NW Rota-1 submarine volcano in the southern Mariana Arc (Butterfield et al., 2011). These fluids are characterized by pH (25 °C) values as low as 1.0, ΣSO_4 concentrations as high as 165 mmol/kg, and aqueous Al concentrations as high as 2.6 mmol/kg (Butterfield et al., 2011). They are likely responsible for the formation of Al- and S-rich hydrothermal plumes in the overlying water column at NW Rota-1 (Resing et al., 2007). Although shallow water depth at NW Rota-1 (520 m) relative to the DESMOS and North Su results in the formation of CO_2-rich gas bubbles and partitioning of magmatic volatiles between liquid water and a gas phase, the fundamental process of magmatic degassing, seawater mixing, and fluid-rock interaction with a highly altered mineral assemblage may be very similar to that occurring in the Manus Basin. Indeed, extrapolation of magmatically derived total dissolved sulfur present in the aqueous phase from the Brimstone vent at NW Rota-1 (Butterfield et al., 2011) to zero Mg yields a magmatic end-member of ~1.1 mol/kg that is similar to the magmatic end-member of 1.2 mol/kg for the D1 vent. The similarity of the NW Rota-1 fluids with those observed at DESMOS and North Su where active eruptions were not observed, suggests that production of acid-sulfate fluids may not be a unique feature of volcanic eruptions, but instead reflects the presence of significant magma accumulations at shallow levels within the ocean crust.

6. IMPLICATIONS AND SUMMARY

The chemistry of acid-sulfate fluids at DESMOS, North Su, and other acid-sulfate systems points to an origin involving the mixing of magmatic volatiles with seawater and chemical interaction with highly altered crustal rocks. The high acidity of these fluids results in intense alteration of the oceanic crust and the aqueous mobilization of metals such as Al that are relatively immobile under more alkaline conditions. Substantial compositional differences between acid-sulfate and black smoker fluids suggest that the influence of acid-sulfate venting on global hydrothermal fluxes may differ significantly. The large enrichments of Al and total S in acid-sulfate fluids from near-arc environments have been used in conjunction with estimates for the arc-associated hydrothermal heat output to estimate the global flux of these species (Butterfield et al., 2011). Results presented here, however, suggest that the volume of acid-sulfate fluids venting in back-arc and arc-environments is ultimately constrained by the volume of magmatic volatiles, not the magmatic heat budget, since the lack of convective hydrothermal circulation limits their ability to mine heat from the oceanic crust. The majority of crustal cooling in back-arc and near-arc environments likely occurs by convective circulation of seawater-derived black-smoker fluids that are also abundantly present in these environments, but contain substantially lower concentrations of Al and S species (Fouquet et al., 1993; Auzende et al., 1996; Gamo et al., 1996a, 1996b; Ishibashi et al., 1996; Douville et al., 1999a,b; Fourre et al., 2006; Takai et al., 2008; Butterfield et al., 2011; Mottl et al., 2011; Reeves et al., 2011). Accordingly, global flux calculations that use hydrothermal heat flux to constrain the mass of acid-sulfate fluids venting in back-arc and arc environments may substantially overestimate the contribution of Al and S to the oceans.

In addition to chemical fluxes to the ocean, the volume of acid-sulfate fluids venting in back-arc and arc environments has important implications for the spatial extent of crustal alteration. Rock composition may be extensively changed during interaction with acid-sulfate fluids due to the efficiency with which cations are leached under highly acidic conditions and is evident in the occurrence of argillic and advanced argillic alteration assemblages where magmatic degassing is prevalent (e.g., Gena et al., 2001). The spatial extent of such alteration, however, is limited by the volume of acid-sulfate fluids and subsurface hydrogeology that regulates fluid flow above a degassing magma chamber. Relative to seawater-derived black-smoker fluids that can access a significant portion of magmatic heat available in a subseafloor magma chamber during convective circulation, the volume of acid-sulfate fluids will likely be substantially smaller. Moreover, the low abundance of mobile trace elements such as Cs, Rb, and Li in acid-sulfate fluids indicates that they have not reacted with large quantities of fresh rock, requiring fluid-rock interaction under fluid-dominated conditions. In contrast, black-smoker fluids from oceanic spreading centers are highly enriched in Cs, Rb, and Li indicating interaction with fresh rock under conditions of low water/rock ratio facilitated by a migrating cracking front (Lister, 1974). Greater volumes of fluid interacting with the crust under conditions of lower/water rock ratio requires that the volumetric extent of crustal alteration by black-smoker fluids is substantially greater than that occurring in response to venting of acid-sulfate fluids.

The role of magmatic volatiles during ore formation has been discussed extensively in the literature (*cf*. Hedenquist and Lowenstern, 1994; Yang and Scott, 1996). Some suggest that magmatic volatiles are enriched in ore-forming metals derived directly from the magma while others suggest that the extreme acidity of these fluids facilitates leaching of ore-forming metals from surrounding rocks. Owing to the trace abundance of ore-forming metals in crustal rocks in back-arc and arc environments, the leaching model requires interaction of acid-sulfate fluids with substantial quantities of crustal rocks. The volume of acid-sulfate fluids may be limited by the availability of magmatic volatiles which, in turn, may limit the volume of crustal rock that undergoes direct leaching by such fluids. However, the addition of acidic magmatic volatiles to convective black smoker fluids, as has been suggested for other back-arc convective hydrothermal systems (de Ronde et al., 2005; de Ronde et al., 2011; Mottl et al., 2011; Reeves et al., 2011) may allow magmatically-derived acidity to access larger volumes of rock and their associated ore-forming metals. The role of magmatically derived vent fluids presented in this study during ore-formation is further complicated by the absence of significant ΣH_2S that precludes precipitation of large quantities of metal sulfides at or below the seafloor, and the absence of a mechanism to titrate the extreme acidity that is necessary to induce precipitation below the seafloor. Indeed, a characteristic trait of the acidic metal-rich fluids venting in places like DESMOS and North Su is the lack of sulfide deposition associated with white smokers. Additional information regarding the abundance of ore-forming metals in acid-sulfate fluids and the extent to which magmatic degassing influences the mobilization of metals in seawater-derived black-smoker fluids is required to better constrain the role of magmatic volatiles during ore-formation processes. On a broader scale, more widespread geochemical characterization of acid-sulfate fluids emanating from volcanic edifices in back-arc and intraoceanic arc settings will allow for a greater understanding of how these fluids influence geochemical fluxes, ocean chemistry and recycling processes associated with subduction.

ACKNOWLEDGEMENTS

We thank the *Jason* group and the crew of the RV *Melville* for their expertise, assistance, and dedication that contributed to a very successful field program. The authors thank Dr. Matthew Leybourne and two anonymous reviewers for their insightful comments that improved the paper. This study received financial support from NSF Grant OCE-0327448, the WHOI Deep Ocean Exploration Institute Graduate Fellowship to E.P. Reeves, the Ocean Drilling Program Schlanger Fellowship to P.R. Craddock and a fellowship from the Hanse-Wissenschaftskolleg to J.S. Seewald.

REFERENCES

Alt J. C. (1995) Subseafloor processes in mid-ocean ridge hydrothermal systems. In *Seafloor Hydrothermal Systems: Physical, Chemical, Biological, and Geological Interactions*, vol. 91 (eds. S. E. Humphris, R. A. Zierenberg, L. S. Mullineaux and R. E. Thomson), pp. 85–114. AGU Monograph. American Geophysical Union.

Alt J. C. and Bach W. (2003) Alteration of oceanic crust: subsurface water-rock interactions. In *Dahlem Workshop Report: Energy and Mass Transfer in Marine Hydrothermal Systems* (eds. P. E. Halbach, V. Tunnicliffe and J. R. Hein). Dahlem University Press.

Alt J. C. and Teagle D. A. H. (1999) The uptake of carbon during alteration of ocean crust. *Geochim. Cosmochim. Acta* **63**, 1527–1535.

Auzende J. M., Urabe T., Ruellan E., Chabroux D., Charlou J. L., Gena K., Gamo T., Henry K., Matsubayashi O. and Matsumoto T., et al. (1996) "Shinkai 6500" dives in the Manus Basin: new STARMER Japanese-French program. *JAMSTEC J. Deep Sea Res.* **12**, 323–334.

Auzende J. M., Hashimoto J., Fialamedioni A. and Ohta S. (1997) In situ geological and biological study of two hydrothermal zones in the Manus Basin (Papua New Guinea). *C.R. Acad. Sci., Ser. IIa: Sci. Terre Planets* **325**(8), 585–591.

Auzende J. M., Ishibashi J., Beaudoin Y., Charlou J. L., Delteil J., Donval J. P., Fouquet Y., Gouillou J. P., Ildefonse B. and Kimura H., et al. (2000) The eastern and western tips of Manus Basin (Papua, New Guinea) explored by submersible; MANAUTE cruise. *C.R. Acad. Sci., Ser. IIa: Sci. Terre Planets* **331**(2), 119–126.

Berndt M. E., Seal R. R., Shanks W. C. and Seyfried, W. E. Jr., (1996) Hydrogen isotope systematics of phase separation in submarine hydrothermal systems: experimental calibration and theoretical models. *Geochim. Cosmochim. Acta* **60**(9), 1595–1604.

Bezos A., Escrig S., Langmuir C. H., Michael P. J. and Asimow P. D. (2009) Origins of chemical diversity of back-arc basin basalts: a segment scale study of the Eastern Lau Spreading Center. *J. Geophys. Res.* **114**, B06212. http://dx.doi.org/10.1029/2008JB005924.

Binns R. A. and Scott S. D. (1993) Actively forming polymetallic sulfide deposits associated with felsic volcanic-rocks in the Eastern Manus Back-Arc Basin, Papua New Guinea. *Econ. Geol.* **88**(8), 2226–2236.

Binns R. A., Scott S. D., Gemmell J. B., Crook K. and Party S. S. (1997) The SuSu Knolls hydrothermal field, Eastern Manus Basin, Papua New Guinea. *EOS Trans. AGU* **78**(722), Fall Meet. Suppl. Abstract V22E-02.

Binns R. A., Barriga F. J. A. S. and Miller D. J. (2007) Leg 193 synthesis: anatomy of an active felsic-hosted hydrothermal system, Eastern Manus Basin, Papua New Guinea. In *Proceedings of the Ocean Drilling Program, Scientific Results*, (eds. F. J. A. S. Barriga, R. A. Binns, D. J. Miller and P. M. Herzig). **193**. pp. 1–71.

Bischoff J. L. and Rosenbauer R. J. (1985) An empirical equation of state for hydrothermal seawater (3.2 percent NaCl). *Am. J. Sci.* **285**, 725–763.

Both R., Crook K., Taylor B., Brogan S., Chappell B., Frankel E., Liu L., Sinton J. and Tiffin D. (1986) Hydrothermal chimneys and associated fauna in the Manus back-arc basin, Papua New Guinea. *EOS Trans. AGU* **67**, 489–491.

Bowers T. S. (1989) Stable isotope signatures of water–rock interaction in mid-ocean ridge hydrothermal systems: sulfur, oxygen and hydrogen. *J. Geophys. Res.* **94**(B5), 5775–5786.

Bowers T. S. and Taylor H. P. (1985) An integrated chemical and stable-isotope model of the origin of midocean ridge hot spring systems. *J. Geophys. Res.* **90**(B14), 12583–12606.

Butterfield D., Seyfried, W. E. Jr., and Lilley M. (2003) Composition and evolution of hydrothermal fluids. In *Dahlem Workshop Report: Energy and Mass Transfer in Marine Hydrothermal Systems*, vol. 89 (eds. P. E. Halbach, V.

Tunnicliffe and J. R. Hein). Dahlem University Press, pp. 123–161.

Butterfield D. A., Nakamura K., Takano B., Lilley M. D., Lupton J. E., Resing J. A. and Roe K. K. (2011) High SO_2 flux, sulfur accumulation, and gas fractionation at an erupting submarine volcano. *Geology* **39**, 803–806.

Caltabiano T., Romano R. and Budetta G. (1994) SO_2 flux measurements at Mount Etna (Sicily). *J. Geophys. Res. Atmos.* **99**, 12809–12819.

Carroll M. R. and Rutherford M. J. (1988) Sulfur speciation in hydrous experimental glasses of varying oxidation state: results from measured wavelength shifts of sulfur X-rays. *Am. Mineral.* **73**, 845–849.

Carroll M. R. and Webster J. D. (1994) Solubilities of sulfur, noble gases, nitrogen, chlorine, and fluorine in magmas. In *Volatiles in Magmas*, vol. 1 (eds. M. R. Carroll and J. R. Holloway), pp. 231–279. Reviews in Mineralogy. Mineralogical Society of America.

Charlou J. L., Donval J. P., Douville E., Jean-Baptiste P., Knoery J., Fouquet Y., Dapoigny A. and Stievenard M. (2000) Compared geochemical signature and evolution of Menez Gwen (37j50VN) and Lucky Strike (37j17VN) hydrothermal fluids, south of the Azores Triple Junction on the Mid-Atlantic Ridge. *Chem. Geol.* **171**, 49–75.

Charlou J. L., Donval J. P., Fouquet Y., Jean-Baptiste P. and Holm N. (2002) Geochemistry of high H_2 and CH_4 vent fluids issuing from ultramafic rocks at the Rainbow hydrothermal field (36°14′N, MAR). *Chem. Geol.* **191**(4), 345–359.

Coltice N., Simon L. and Lecuyer C. (2004) Carbon isotope cycle and mantle structure. *Geophys. Res. Lett.* **31**(5), L05603. http://dx.doi.org/10.1029/2003GL018873.

Craddock P. R., Bach W., Seewald J. S., Rouxel O. J., Reeves E. and Tivey M. K. (2010) Rare earth element abundances in hydrothermal fluids from the Manus Basin, Papua New Guinea: indicators of sub-seafloor hydrothermal processes in back-arc basins. *Geochim. Cosmochim. Acta* **74**, 5494–5513.

Craig H. (1970) Abyssal carbon-13 in the South Pacific. *J. Geophys. Res.* **75**(3), 691–695.

Craig H. and Gordon L. I. (1965) Deuterium and oxygen 18 variations in the ocean and marine atmosphere. In *Stable Isotopes in Oceanographic Studies and Paleotemperatures* (ed. E. Tongiogi). Consiglio Nazionale Delle Ricerche, Laboratorio Di Geologia Nucleare, Pisa, pp. 9–130.

Crook K. (1987) Petrology and mineral chemistry of sedimentary rocks from the Western Solomon Sea. *Geo-Mar. Lett.* **6**, 203–209.

de Ronde C. E. J. (1995) Fluid chemistry and isotopic characteristics of seafloor hydrothermal systems and associated VMS deposits: potential for magmatic contribution. In *Magmas, Fluids, and Ore Deposits* (ed. J. F. H. Thompson). Mineralogical Association of Canada, Victoria, British Columbia, pp. 479–509.

de Ronde C. E. J., Massoth G. J., Butterfield D. A., Christenson B. W., Ishibashi J., Ditchburn R. G., Hannington M. D., Brathwaite R. L., Lupton J. E., Kamenetsky V. S. and Graham I. J., et al. (2011) Submarine hydrothermal activity and gold-rich mineralization at Brothers Volcano, Kermadec Arc, New Zealand. *Miner. Deposita* **46**, 541–584.

de Ronde C. E. J., Massoth G. J., Barker E. T. and Lupton J. E. (2003) Submarine hydrothermal venting related to volcanic arcs. In (eds. S. F. Simmons and I. Graham). Society of Economic Geologists, Inc., Special Publication. pp 91–110.

de Ronde C. E. J., Hannington M. D., Stoffers P., Wright I. C., Ditchburn R. G., Reyes A. G., Baker E. T., Massoth G. J., Lupton J. E. and Walker S. L., et al. (2005) Evolution of a submarine magmatic–hydrothermal system: brothers volcano, southern Kermadec arc, New Zealand. *Econ. Geol.* **100**(6), 1097–1133.

Douville E., Bienvenu P., Charlou J. L., Donval J. P., Fouquet Y., Appriou P. and Gamo T. (1999a) Yttrium and rare earth elements in fluids from various deep-sea hydrothermal systems. *Geochim. Cosmochim. Acta* **63**(5), 627–643.

Douville E., Charlou J. L., Donval J. P., Hureau D. and Appriou P. (1999b) As and Sb behaviour in fluids from various deep-sea hydrothermal systems. *C.R. Acad. Sci., Ser. IIa: Sci. Terre Planets* **328**(2), 97–104.

Drummond S. E. (1981) Boiling and mixing of hydrothermal fluids: chemical effects on mineral precipitation, Ph. D. dissertation, Penn. State University.

Eickmann B., Bach W., Rosner M. and Peckmann J. (2009) Geochemical constraints on the modes of carbonate precipitation in peridotites from the Logatchev Hydrothermal Vent Field and Gakkel Ridge. *Chem. Geol.* **268**(1–2), 97–106.

Embley R. W., Chadwick W. W., Baker E. T., Butterfield D. A., Resing J. A., De Ronde C. E. J., Tunnicliffe V., Lupton J. E., Juniper S. K. and Rubin K. H., et al. (2006) Long-term eruptive activity at a submarine arc volcano. *Nature* **441**(7092), 494–497.

Escrig S., Bezos A., Goldstein S. L., Langmuir C. H. and Michael P. J. (2009) Mantle source variations beneath the Eastern Lau Spreading Center and the nature of subduction components in the Lau Basin-Tonga arc system. *Geochem. Geophys. Geosyst.* **10**, Q04014. http://dx.doi.org/10.1029/2008GC002281.

Fouquet Y., Vonstackelberg U., Charlou J. L., Erzinger J., Herzig P. M., Muhe R. and Wiedicke M. (1993) Metallogenesis in back-arc environments – the Lau Basin example. *Econ. Geol.* **88**(8), 2154–2181.

Fourre E., Jean-Baptiste P., Charlou J. L., Donval J. P. and Ishibashi J. I. (2006) Helium isotopic composition of hydrothermal fluids from the Manus back-arc Basin, Papua New Guinea. *Geochem. J.* **40**, 245–252.

Gamo T., Sakai H., Ishibashi J., Nakayama E., Isshiki K., Matsuura H., Shitashima K., Takeuchi K. and Ohta S. (1993) Hydrothermal plumes in the Eastern Manus Basin, Bismarck Sea – CH_4, Mn, Al and pH anomalies. *Deep-Sea Res. Part I* **40**(11–12), 2335–2349.

Gamo T., Okamura K., Charlou J. L., Urabe T., Auzende J. M., Cruise S. S. P. O. T. M., Ishibashi J., Shitashima K. and Kodama Y. (1996a) Chemical exploration of hydrothermal activity in the Manus Basin, Papua New Guinea (ManusFlux Cruise). *JAMSTEC J. Deep Sea Res.* **12**, 335–345.

Gamo T., Okamura K., Kodama T., Charlou J. L., Urabe T., Auzende J. M., Ishibashi J. and Party A. T. S. S. (1996b) Chemical characteristics of hydrothermal fluids from the Manus back-arc basin, Papua New Guinea, I. Major chemical components. *EOS Trans. AGU* **77**(W116), WPGM Suppl. Abstract T32A-5.

Gamo T., Okamura K., Charlou J. L., Urabe T., Auzende J. M., Ishibashi J., Shitashima K. and Chiba H. (1997) Acidic and sulfate-rich hydrothermal fluids from the Manus back-arc basin, Papua New Guinea. *Geology* **25**(2), 139–142.

Gamo T., Ishibashi J., Tsunogai U., Okamura K. and Chiba H. (2006) Unique geochemistry of submarine hydrothermal fluids from arc-back-arc settings of the Western Pacific. In *Back-Arc Spreading Systems: Geological, Biological, Chemical, and Physical Interactions*, vol. 166 (eds. D. M. Christie, C. R. Fisher, S.-M. Lee and S. Givens), pp. 147–161. AGU Monograph. American Geophysical Union.

Gena K., Mizuta T., Ishiyama D. and Urabe T. (2001) Acid-sulphate type alteration and mineralization in the DESMOS caldera, Manus back-arc basin, Papua New Guinea. *Resour. Geol.* **51**, 31–44.

Gena K. R., Chiba H., Mizuta T. and Matsubaya O. (2006) Hydrogen, oxygen and sulfur isotope studies of seafloor hydrothermal system at the Desmos caldera, Manus back-arc basin, Papua New Guinea: an analogue of terrestrial acid hot crater-lake. *Resour. Geol.* **56**, 183–190.

German C. and Von Damm K. L. (2003) Hydrothermal processes. In *The Treatise on Geochemistry*, vol. 6 (eds. K. K. Turekian and H. D. Holland). Elsevier, pp. 181–222.

Giggenbach W. F. (1992) Isotopic shifts in waters from geothermal and volcanic systems along convergent plate boundaries and their origin. *Earth Planet. Sci. Lett.* **113**, 495–510.

Giggenbach W. F. (1997) The origin and evolution of fluids in magmatic–hydrothermal systems. In *Geochemistry of Hydrothermal Ore Deposits* (ed. H. L. Barnes). Wiley, pp. 737–796.

Gruen G., Weis P., Driesner T., Heinrich C. A. and de Ronde C. E. J. (2014) Hydrodynamic modeling of magmatic–hydrothermal activity at submarine arc volcanoes, with implications for ore formation.

Hedenquist J. W., Aoki M. and Shinohara H. (1994) Flux of volatiles and ore-forming metals from the magmatic–hydrothermal system of satsuma Iwojima volcano. *Geology* **22**, 585–588.

Hedenquist J. W. and Lowenstern J. B. (1994) The role of magmas in the formation of hydrothermal ore deposits. *Nature* **370**, 519–527.

Heinrich C. A. (2005) The physical and chemical evolution of low-salinity magmatic fluids at the porphyry to epithermal transition: a thermodynamic study. *Miner. Deposita* **39**, 864–889.

Helgeson H. C., Delany J. M., Nesbitt H. W. and Bird D. K. (1978) Summary and critique of the thermodynamic properties of rock-forming minerals. *Am. J. Sci.* **278A**, 1–229.

Helgeson H. C., Kirkham D. H. and Flowers G. C. (1981) Theoretical prediction of the thermodynamic behavior of aqueous electrolytes at high pressures and temperatures. IV. Calculation of activity coefficients, osmotic coefficients, and apparent molal and standard and relative partial molal properties to 5 kb and 600 °C. *Am. J. Sci.* **281**, 1241–1516.

Holland H. D. (1965) Some applications of thermochemical data to problems in ore deposits II. Mineral assemblages and the composition of ore-forming fluids. *Econ. Geol.* **60**, 1101–1166.

Holland H. D. and Malinin S. D. (1979) The solubility and occurrence of non-ore minerals. In *Geochemistry of Hydrothermal Ore Deposits* (ed. H. L. Barnes). Wiley, pp. 461–508.

Holloway J. R. and Blank J. G. (1994) Application of experimental results to C–O–H species in natural melts. *Volatiles in Magmas* **30**, 187–230.

Hrischeva E., Scott S. D. and Weston R. (2007) Metalliferous sediments associated with presently forming volcanogenic massive sulfides: the SuSu Knolls hydrothermal field, Eastern Manus Basin, Papua New Guinea. *Econ. Geol.* **102**(1), 55–73.

Huss, Jr., A., Lim P. K. and Eckert C. A. (1982) Oxidation of aqueous sulfur dioxide. 1. Homogeneous manganese(II) and iron(II) catalysis at low pH. *J. Phys. Chem.* **86**, 4224–4228.

Ishibashi J., Wakita K., Okamura K., Gamo T., Shitashima K., Charlou J. L., Donval J. P., Jean-Baptiste P. and Party A. T. S. S. (1996) Chemical characteristics of hydrothermal fluids from the Manus back-arc basin, Papua New Guinea, II. Gas components. *EOS Trans. AGU* **77**(W116), WPGM Suppl. Abstract T32A-6.

Iwasaki I. and Ozawa T. (1960) Genesis of sulfate in acid hot spring. *Bull. Chem. Soc. Jpn.* **33**, 1018–1019.

Johnson J. W., Oelkers E. H. and Helgeson H. C. (1992) SUPCRT92: a software package for calculating the standard molal thermodynamic properties of minerals, gases, aqueous species, and reactions from 1 to 5000 bar and 0 to 1000 °C. *Comput. Geosci.* **18**, 899–947.

Kamenetsky V. S., Binns R. A., Gemmell J. B., Crawford A. J., Mernagh T. P., Maas R. and Steele D. (2001) Parental basaltic melts and fluids in eastern Manus backarc basin: implications for hydrothermal mineralisation. *Earth Planet. Sci. Lett.* **184**, 685–702.

Kelley D. S., Lilley M. D. and Früh-Green G. L. (2004) Volatiles in submarine environments: food for life. In *The Subseafloor Biosphere at Mid-Ocean Ridges*, vol. 144 (eds. W. S. D. Wilcock, E. F. DeLong, D. S. Kelley, J. A. Baross and S. C. Cary), pp. 167–189. AGU Monograph. American Geophysical Union.

Kendall C. and Coplen T. B. (1985) Multisample conversion of water to hydrogen by zinc for stable isotope determination. *Anal. Chem.* **57**(7), 1437–1440.

Kusakabe M., Komoda Y., Takano B. and Abiko T. (2000) Sulfur isotopic effects in the disproportionation reaction of sulfur dioxide in hydrothermal fluids: implications for the $\delta^{34}S$ variations of dissolved bisulfate and elemental sulfur from active crater lakes. *J. Volcanol. Geoth. Res.* **97**, 287–307.

Lackschewitz K. S., Devey C. W., Stoffers P., Botz R., Eisenhauer A., Kummetz M., Schmidt M. and Singer A. (2004) Mineralogical, geochemical and isotopic characteristics of hydrothermal alteration processes in the active, submarine, felsic-hosted PACMANUS field, Manus Basin, Papua New Guinea. *Geochim. Cosmochim. Acta* **68**(21), 4405–4427.

Lee S. M. and Ruellan E. (2006) Tectonic and magmatic evolution of the Bismarck Sea, Papua New Guinea: review and new synthesis. In *Back-Arc Spreading Systems: Geological, Biological, Chemical, and Physical Interactions*, vol. 166 (eds. D. M. Christie, C. R. Fisher, S.-M. Lee and S. Givens), pp. 263–286. AGU Monograph. American Geophysical Union.

Leybourne M. I., Schwarz-Schampera U., de Ronde C. E. J., Baker E. T., Faure K., Walker S. L., Butterfield D. A., Resing J. A., Lupton J. E., Hannington M. D., Gibson H. L., Massoth G. J., Embley R. W., Chadwick W. W., Clark M. R., Timm C., Graham I. J. and Wright I. C. (2012) Submarine magmatic–hydrothermal systems at the Monowai Volcanic Center, Kermadec Arc. *Econ. Geol.* **107**, 1669–1694.

Lilley M. D., Butterfield D. A., Lupton J. E. and Olson E. J. (2003) Magmatic events can produce rapid changes in hydrothermal vent chemistry. *Nature* **422**(6934), 878–881.

Linstrom, P. J. and Mallard, W. G. (eds.) (2014) *NIST Chemistry WebBook, NIST Standard Reference Database Number 69*. National Institute of Standards and Technology, Gaithersburg MD, 20899, <http://webbook.nist.gov>, (retrieved September 29, 2014).

Lisitsyn A. P., Crook K., Bogdanov Y. A., Zonenshain L. P., Murav'yev K. G., Tufar W., Gurvich Y. G., Gordeyev V. V. and Ivanov G. V. (1993) A hydrothermal field in the rift zone of the Manus Basin, Bismarck Sea. *Int. Geol. Rev.* **35**(2), 105–126.

Lister C. R. B. (1974) On the penetration of water into hot rock. *Geophys. J. Roy. Astron. Soc.* **39**, 465–509.

Lister C. R. B. (1983) On the intermittency and crystallization mechanisms of sub-seafloor magma chambers. *Geophys. J. Roy. Astron. Soc.* **73**(2), 351–365.

Martinez F. and Taylor B. (1996) Backarc spreading, rifting, and microplate rotation, between transform faults in the Manus basin. *Mar. Geophys. Res.* **18**(2–4), 203–224.

Martinez F., Taylor B., Baker E. T., Resing J. A. and Walker S. L. (2006) Opposing trends in crustal thickness and spreading rate along the back-arc Eastern Lau Spreading Center: implications for controls on ridge morphology, faulting, and hydrothermal activity. *Earth Planet. Sci. Lett.* **245**, 655–672. http://dx.doi.org/10.1016/j.epsl.2006.03.049.

McDermott J. M., Ono S., Tivey M. K., Seewald J., Shanks W. C. and Solow, III, A. R. (2015) Identification of sulfur sources and isotopic equilibria in submarine hot-springs using multiple sulfur isotopes. *Geochim. Cosmoshim. Acta* **160**, 169–187.

Moss R. and Scott S. D. (2001) Geochemistry and mineralogy of gold-rich hydrothermal precipitates from the eastern Manus Basin, Papua New Guinea. *Can. Mineral.* **39**, 957–978.

Mottl M. J., Seewald J. S., Wheat C. G., Tivey M. K., Michael P. J., Proskurowski G., McCollom T. M., Reeves E., Sharkey J., You C. F., Chan L. H. and Pichler T. (2011) Chemistry of hot springs along the Eastern Lau Spreading Center. *Geochim. Cosmochim. Acta* **75**, 1013–1038.

Ohmoto H. (1986) Stable isotope geochemistry of ore deposits. In *Stable Isotopes in High Temperature Geological Processes*, vol. 16 (eds. J. W. Valley, H. P. Taylor and J. R. O'Neil), pp. 491–559. Reviews in Mineralogy. Mineralogical Society of America.

Ohmoto H. and Lasaga A. C. (1982) Kinetics of reactions between aqueous sulfates and sulfides in hydrothermal systems. *Geochim. Cosmochim. Acta* **46**, 1727–1745.

Park S. H., Lee S.-M., Kamenov G. D., Kwon S.-T. and Lee K.-Y. (2010) Tracing the origin of subduction components beneath the South East rift in the Manus Basin, Papua New Guinea. *Chem. Geol.* **269**, 339–349.

Paulick H. and Bach W. (2006) Phyllosilicate mineralogy of the submarine, dacite-hosted, Pacmanus hydrothermal system – integration of SWIR, XRD, and geochemical data (Papua New Guinea, ODP Leg 193). *Econ. Geol.* **101**, 633–650.

Pearce J. A. and Stern R. J. (2006) Origin of back-arc basin magmas: trace element and isotope perspectives. In *Back-Arc Spreading Systems: Geological, Biological, Chemical, and Physical Interactions* (eds. D. M. Christie, C. R. Fisher, S.-M. Lee and S. Givens), pp. 63–86. AGU Monograph. American Geophysical Union.

Pérez N. M., Wakita H., Lolok D., Patia H., Talai B. and McKee C. O. (1996) Anomalous soil gas CO_2 concentrations and relation to seismic activity at Rabaul caldera, Papua New Guinea. *Geogaceta* **20**(4), 1000–1003.

Pester N. J., Reeves E. P., Rough M. E., Ding K., Seewald J. S. and Seyfried, Jr., W. E. (2012) Subseafloor phase equilibria in high-temperature hydrothermal fluids of the Lucky Strike Seamount (Mid-Atlantic Ridge, 37°17′N). *Geochim. Cosmochim. Acta* **90**, 303–322.

Proskurowski G., Seewald J. S., Reeves E., McCollom T. M., Lupton J., Sylva S. P. and Tivey M. K. (2007) Volatile chemistry at Lau Basin hydrothermal sites: basin-wide trends of slab carbonate influence and suggestions of abiotic methane oxidation at the Mariner vent site. *EOS Trans. AGU* **88**(52), Fall Meet. Suppl. V34B-04.

Rees C. E., Jenkins W. J. and Monster J. (1978) Sulfur isotopic composition of ocean water sulfate. *Geochim. Cosmochim. Acta* **42**, 377–381.

Reeves E. P., Seewald J. S., Saccocia P., Bach W., Craddock P. R., Shanks W. C., Sylva S. P., Walsh E., Pichler T. and Rosner M. (2011) Geochemistry of hydrothermal fluids from the PACMANUS, Northeast Pual and Vienna Woods hydrothermal fields, Manus Basin, Papua New Guinea. *Geochim. Cosmochim. Acta* **75**, 1088–1123.

Redfield K. H. and Scott S. D. (1965) Factors affecting the distribution of deuterium in the ocean. In *Symposium on Marine Geochemistr. Occasional Publication*, vol. 3 (eds. D. R. Schink and J. T. Corless), pp. 149–168. AGU Monograph. Narragansett Marine Laboratory, University of Rhode Island.

Resing J. A., Lebon G., Baker E. T., Lupton J. E., Embley R. W., Massoth G. J., Chadwick W. W. and De Ronde C. E. J. (2007) Venting of acid-sulfate fluids in a high-sulfidation setting at NW Rota-1 submarine volcano on the Mariana Arc. *Econ. Geol.* **102**, 1047–1061.

Sarmiento J. L. and Gruber N. (2006) Ocean Biogeochemical Dynamics, Princeton University Press.

Scaillet B. and Pichavant M. (2003) Experimental constraints on volatile abundances in arc magmas and their implications for degassing processes. *Geol. Soc. Lond., Spec. Publ.* **213**, 23–52.

Seewald J. S. and Seyfried, Jr., W. E. (1990) The effect of temperature on heavy and base metal mobility in subseafloor hydrothermal systems: constraints from basalt alteration experiments and field studies. *Earth Planet. Sci. Lett.* **101**, 388–403.

Seewald J. S., Seyfried, Jr., W. E. and Thornton E. C. (1990) Organic-rich sediment alteration: an experimental and theoretical study at elevated temperatures and pressures. *Appl. Geochem.* **5**, 193–209.

Seewald J. S., Doherty K. W., Hammar T. R. and Liberatore S. P. (2002) A new gas-tight isobaric sampler for hydrothermal fluids. *Deep-Sea Res. Part I* **49**(1), 189–196.

Seewald J., Cruse A. and Saccocia P. (2003) Aqueous volatiles in hydrothermal fluids from the Main Endeavour Field, northern Juan de Fuca Ridge: temporal variability following earthquake activity. *Earth Planet. Sci. Lett.* **216**(4), 575–590.

Seewald J. S., Seyfried, Jr., W. E. and Shanks, III, W. C. (1994) Variations in the chemical and stable isotope composition of carbon and sulfur species during organic-rich sediment alteration: an experimental and theoretical study of hydrothermal activity at Guaymas Basin, Gulf of California. *Geochim. Cosmochim. Acta* **58**, 5065–5082.

Seyfried, W. E. Jr., (1987) Experimental and theoretical constraints on hydrothermal alteration processes at mid-ocean ridges. *Annu. Rev. Earth Planet. Sci.* **15**, 317–335.

Seyfried, W. E. Jr., and Ding K. (1995) The hydrothermal chemistry of fluoride in seawater. *Geochim. Cosmochim. Acta* **59**(6), 1063–1071.

Shanks, III, W. C. (2001) Stable isotopes in seafloor hydrothermal systems: vent fluids, hydrothermal deposits, hydrothermal alteration, and microbial processes. *Rev. Mineral. Geochem.* **43**, 469–525.

Shanks, III, W. C., Böhlke J. K. and Seal R. R. (1995) Stable isotopes in mid-ocean ridge hydrothermal systems: interactions between fluids, minerals, and organisms. In *Seafloor Hydrothermal Systems: Physical, Chemical, Biological, and Geological Interactions*, vol. 91 (eds. S. E. Humphris, R. A. Zierenberg, L. S. Mullineaux and R. E. Thomson), pp. 194–221. AGU Monograph. American Geophysical Union.

Shaw A. M., Hauri E. H., Fischer T. P., Hilton D. R. and Kelley K. A. (2008) Hydrogen isotopes in Mariana arc melt inclusions: implications for subduction dehydration and the deep-Earth water cycle. *Earth Planet. Sci. Lett.* **275**, 138–145.

Shock E. L. and Helgeson H. C. (1988) Calculation of the thermodynamic and transport properties of aqueous species at high pressures and temperatures: correlation algorithms for ionic species and equation of state predictions to 5 kb and 1000 °C. *Geochim. Cosmochim. Acta* **52**, 2009–2036.

Shock E. L., Helgeson H. C. and Sverjensky D. A. (1989) Calculation of the thermodynamic and transport properties of aqueous species at high pressures and temperatures: standard partial molal properties of inorganic neutral species. *Geochim. Cosmochim. Acta* **53**, 2157–2183.

Shock E. L., Sassani D. C., Willis M. and Sverjensky D. A. (1997) Inorganic species in geologic fluids: correlations among standard molal thermodynamic properties of aqueous ions and hydroxide complexes. *Geochim. Cosmochim. Acta* **61**, 907–950.

Sinton J. M., Ford L. L., Chappell B. and McCulloch M. T. (2003) Magma genesis and mantle heterogeneity in the Manus back-arc basin, Papua New Guinea. *J. Petrol.* **44**, 159–195.

Spencer D. W., Robertson D. E., Turekian K. K. and Folsom T. R. (1970) Trace element calibrations and profiles at the GEOSECS test station in the Northeast Pacific Ocean. *J. Geophys. Res.* **75**(36), 7688–7696.

Sun W. D., Arculus R. J., Kamenetsky V. S. and Binns R. A. (2004) Release of gold-bearing fluids in convergent margin magmas prompted by magnetite crystallization. *Nature* **431**(7011), 975–978.

Sverjensky D. A., Shock E. L. and Helgeson H. C. (1997) Prediction of the thermodynamic properties of aqueous metal complexes to 1000 °C and 5 kb. *Geochim. Cosmochim. Acta* **61**, 1359–1412.

Tagirov B. and Schott J. (2001) Aluminum speciation in crustal fluids revisited. *Geochim. Cosmochim. Acta* **65**, 3965–3992.

Takai K., Nunoura T., Ishibashi J. I., Lupton J., Suzuki R., Hamasaki H., Ueno Y., Kawagucci S., Gamo T. and Suzuki Y., et al. (2008) Variability in the microbial communities and hydrothermal fluid chemistry at the newly discovered Mariner hydrothermal field, southern Lau Basin. *J. Geophys. Res. Biogeosci.* **113**(G02031). http://dx.doi.org/10.1029/2007JG000636.

Taylor B. (1979a) Bismarck Sea: evolution of a back-arc basin. *Geology* **7**(171–174).

Taylor H. P. (1979b) Oxygen and hydrogen isotope relationships in hydrothermal mineral deposits. In *Geochemistry of Hydrothermal Ore Deposits* (ed. H. L. Barnes). Wiley, pp. 236–277.

Taylor H. P. (1986) Magmatic volatiles: isotopic variation of C, H, and S. In *Stable Isotopes in High Temperature Geological Processes*, vol. 16 (eds. J. W. Valley, H. P. Taylor and J. R. O'Neil), pp. 185–225. Reviews in Mineralogy. Mineralogical Society of America.

Taylor B., Crook K. and Sinton J. (1994) Extensional transform zones and oblique spreading centers. *J. Geophys. Res. Solid Earth* **99**(B10), 19707–19718.

Tivey M., Bach W., Seewald J., Tivey M. K., Vanko D. A. and the Shipboard Science J. I. A. A. T. T. (2006) *Cruise Report for R/V Melville cruise MGLN06MV – Hydrothermal systems in the Eastern Manus Basin: Fluid Chemistry and Magnetic Structure as Guides to Subseafloor Processes*. Woods Hole Oceanographic Institution (available upon request to authors).

Trefry J. H., Butterfield D. B., Metz S., Massoth G. J., Trocine R. P. and Feely R. A. (1994) Trace metals in hydrothermal solutions from cleft segment on the southern Juan De Fuca Ridge. *J. Geophys. Res. Solid Earth* **99**, 4925–4935.

Tregoning P. (2002) Plate kinematics in the western Pacific derived from geodetic observations. *J. Geophys. Res. Solid Earth* **107**(B1).

Tufar W. (1990) Modern hydrothermal activity, formation of complex massive sulfide deposits and associated vent communities in the Manus Back-arc Basin (Bismarck Sea, Papua New Guinea). *Mitt. Osterr. Geol. Ges.* **82**, 183–210.

Von Damm K. L. (1995) Controls on the chemistry and temporal variability of seafloor hydrothermal systems. In *Seafloor Hydrothermal Systems: Physical, Chemical, Biological, and Geological Interactions*, vol. 91 (eds. S. E. Humphris, R. A. Zierenberg, L. S. Mullineaux and R. E. Thomson), pp. 222–247. AGU Monograph. American Geophysical Union.

Von Damm K. L., Edmond J. M., Grant B. and Measures C. I. (1985) Chemistry of submarine hydrothermal solutions at 21°N, East Pacific Rise. *Geochim. Cosmochim. Acta* **49**(11), 2197–2220.

Wolery T. J. (1992) *EQ3NR, A Computer Program for Aqueous Speciation-Solubility Calculations: Theoretical Manual, Users's Guide, and related Documentation*. Lawrence Livermore National Lab.

Yang K. H. and Scott S. D. (1996) Possible contribution of a metal-rich magmatic fluid to a sea-floor hydrothermal system. *Nature* **383**, 420–423.

Yang K. H. and Scott S. D. (2002) Magmatic degassing of volatiles and ore metals into a hydrothermal system on the modern sea floor of the eastern Manus back-arc basin, western Pacific. *Econ. Geol.* **97**, 1079–1100.

Yang K. H. and Scott S. D. (2006) Magmatic fluids as a source of metals in seafloor hydrothermal systems. In *Back-Arc Spreading Systems: Geological, Biological, Chemical, and Physical Interactions*, vol. 166 (eds. D. M. Christie, C. R. Fisher, S.-M. Lee and S. Givens), pp. 163–184. AGU Monograph. American Geophysical Union.

Associate editor: S. Jun-ichiro Ishibashi